CERN 87-13
Proton Synchrotron
Machine Division
14 December 1987

ORGANISATION EUROPÉENNE POUR LA RECHERCHE NUCLÉAIRE
CERN EUROPEAN ORGANIZATION FOR NUCLEAR RESEARCH

PSEUDOSPARK SWITCHES

P. Billault, H. Riege and M. van Gulik
CERN, Geneva, Switzerland

E. Boggasch and K. Frank
Phys. Inst., University of Erlangen-Nürnberg,
Erlangen, Fed. Rep. Germany

R. Seeböck
Siemens AG, Erlangen, Fed. Rep. Germany

GENEVA
1987

ISSN 0007-8328

I—Service d'information scientifique—RD/752-3000-décembre 1987

ABSTRACT

The pseudospark discharge is bound to a geometrical structure which is particularly well suited for switching high currents and voltages at high power levels. This type of discharge offers the potential for improvement in essentially all areas of switching operation: peak current and current density, current rise, stand-off voltage, reverse current capability, cathode life, and forward drop. The first pseudospark switch was built at CERN in 1981. Since then, the basic switching characteristics of pseudospark chambers have been studied in detail. The main feature of a pseudospark switch is the confinement of the discharge plasma to the device axis. The current transition to the hollow electrodes is spread over a rather large surface area. Another essential feature is the easy and precise triggering of the pseudospark switch from the interior of the hollow electrodes, relatively far from the main discharge gap. Nanosecond delay and jitter values can be achieved with trigger energies of less than 0.1 mJ, although cathode heating is not required. Pseudospark gaps may cover a wide range of high-voltage, high-current, and high-pulse-power switching at repetition rates of many kilohertz. This report reviews the basic research on pseudospark switches which has been going on at CERN.

So far, applications have been developed in the range of thyratron-like medium-power switches at typically 20 to 40 kV and 0.5 to 10 kA. High-current pseudospark switches have been built for a high-power 20 kJ pulse generator which is being used for long-term tests of plasma lenses developed for the future CERN Antiproton Collector (ACOL). The high-current switches have operated for several hundred thousand shots, with 20 to 50 ns jitter at 16 kV charging voltage and more than 100 kA peak current amplitude.

CONTENTS

1. INTRODUCTION

In 1889, F. Paschen found the law of electrical breakdown to be valid in gases between two metallic plane electrodes. Figure 1 shows the breakdown voltage as a function of the product of electrode distance d and gas pressure p. In general, the breakdown voltage goes through a minimum, which is the region of glow discharge. The high-pressure branch describes the well-known high-pressure spark. However, fast breakdown can be observed also on the left, low-pressure branch of the Paschen curve. The pseudospark is a phenomenon which takes place in this left-hand region. It is generated in a special geometry, still between two metallic plane electrodes, but owing to Paschen's law it is forced to start on the axis of the centre holes in the hollow electrodes. External long path breakdown is avoided by the use of appropriate insulators (Fig. 2).

First indications for the pseudospark were found in the early fifties by Christiansen [1, 2], during the development of plate counters for nuclear physics experiments. Near the Paschen minimum, anomalous sparks in the edge zones of these counters disturbed the measuring process. Twenty years later, Christiansen and Schultheiss [3] recommenced research into this almost forgotten effect. Transferring the discharge channel from the edges to the centre, by using the trick of centre holes in the electrodes, opened up the way to making a thorough study of the pseudospark. Soon it was realized that the pseudospark chamber (PSC) is a very general device in low-pressure gas discharge physics, in some ways comparable to the laser in optics or the transistor in electronics [4].

The pseudospark discharge is characterized by a very rapid breakdown phase during which high-density particle beams can be extracted from either side of the discharge chamber. The discharge operates with an anomalously high, cold-cathode emission, which is much higher than the emission from a standard hot cathode. Nevertheless, the discharge is seen as a glow rather than an arc. Apart from switching applications, the PSC is a source of high-density beams of electrons [4] and ions [5]. Moreover, highly charged ions can be extracted from the anode plasma, which is formed by the energetic electron beam [4, 6]. Indirectly, the PSC may also generate VUV laser radiation [7], microwaves [8], and ultra-short X-ray flashes [9]. With yields of more than 10^7 K-shell X-ray photons

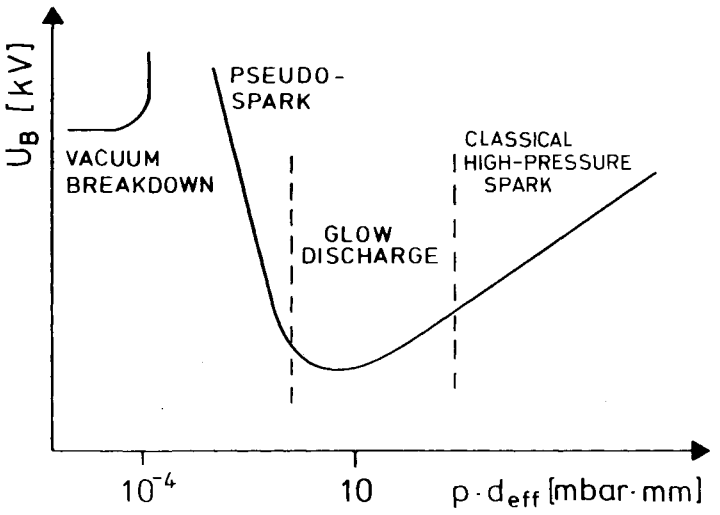

Fig. 1 Typical Paschen curve

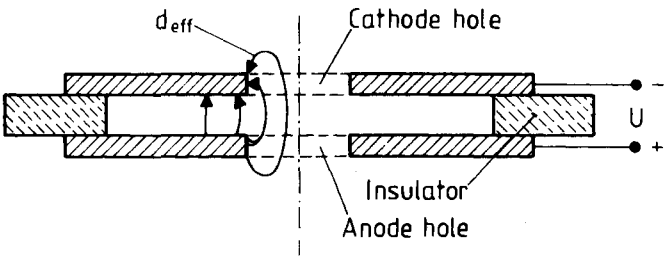

Fig. 2 Basic scheme of a single-gap pseudospark chamber

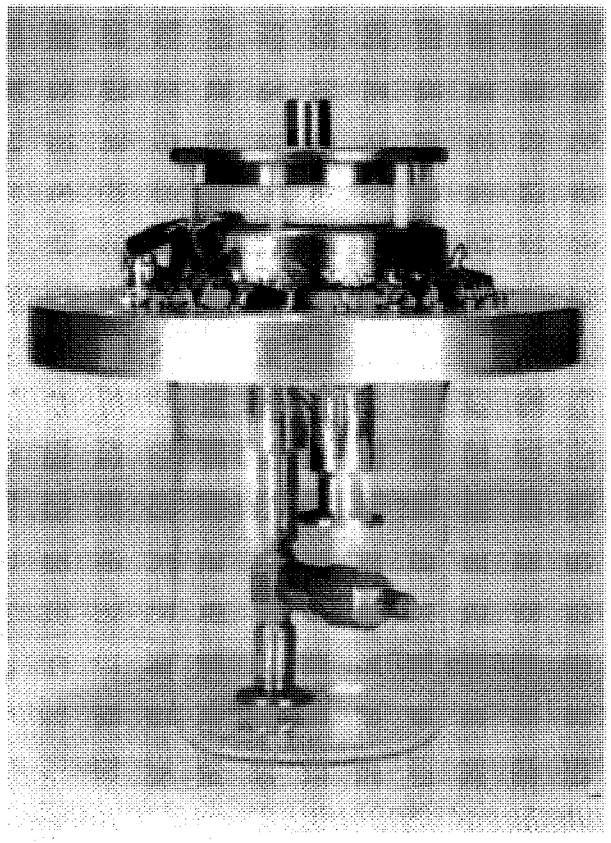

Fig. 3 The first pseudospark switch built at CERN

per nanosecond which have been measured at CERN, the electron beams coming from a PSC and hitting a heavy metal target are amongst the most efficient of the known pulsed sources of soft X-rays.

In 1980, discussions were held at CERN regarding the potential replacement of commercial thyratrons by spark-gap switches. The advantages of spark gaps, however, did not seem great enough to justify any special developments. At that time it seemed worth while to test the switching properties of PSCs, which, owing to their basic structure, were promising for use in high-power switching. A first prototype pseudospark switch (PSS) was built at CERN in 1981 [4]. This very simple experimental switch (Fig. 3) worked, from the start, at 30 kV charging voltage, with current rise-times of about 5–10 ns and a precision of better than ± 1 ns. The excellent results obtained with the prototype encouraged us to propose a limited research programme. The main objectives were: the study of the basic pseudospark physics that are important for switching applications; the systematic development of trigger methods; and the investigation of application ranges in high-current, high-voltage, and high-pulse-power switching.

The main purpose of this report is to review the basic research work done on PSSs at CERN. A few applications developed in our laboratory and elsewhere are also described. A comparison of PSSs with commercial switches—including ignitrons, thyratrons, and high-pressure and vacuum spark gaps—is attempted. Future applications for PSSs, especially in accelerator technology, are proposed.

2. PRINCIPLES OF THE PSEUDOSPARK DISCHARGE

The physical mechanisms of the pseudospark are not yet fully understood. Since the pseudospark occurs on the low-pressure side of the Paschen curve (Fig. 1), anode-directed electron avalanches alone cannot explain the rapid rise in current. The pseudospark discharge takes place not only in a single gap but also in multiple-gap chambers with many floating electrodes. In both cases a luminous plasma 'bubble' is visible in the interior of the hollow cathode (Fig. 4a–d). The build-up of the plasma bubble is favoured by electric field penetration through the cathode hole and by positive

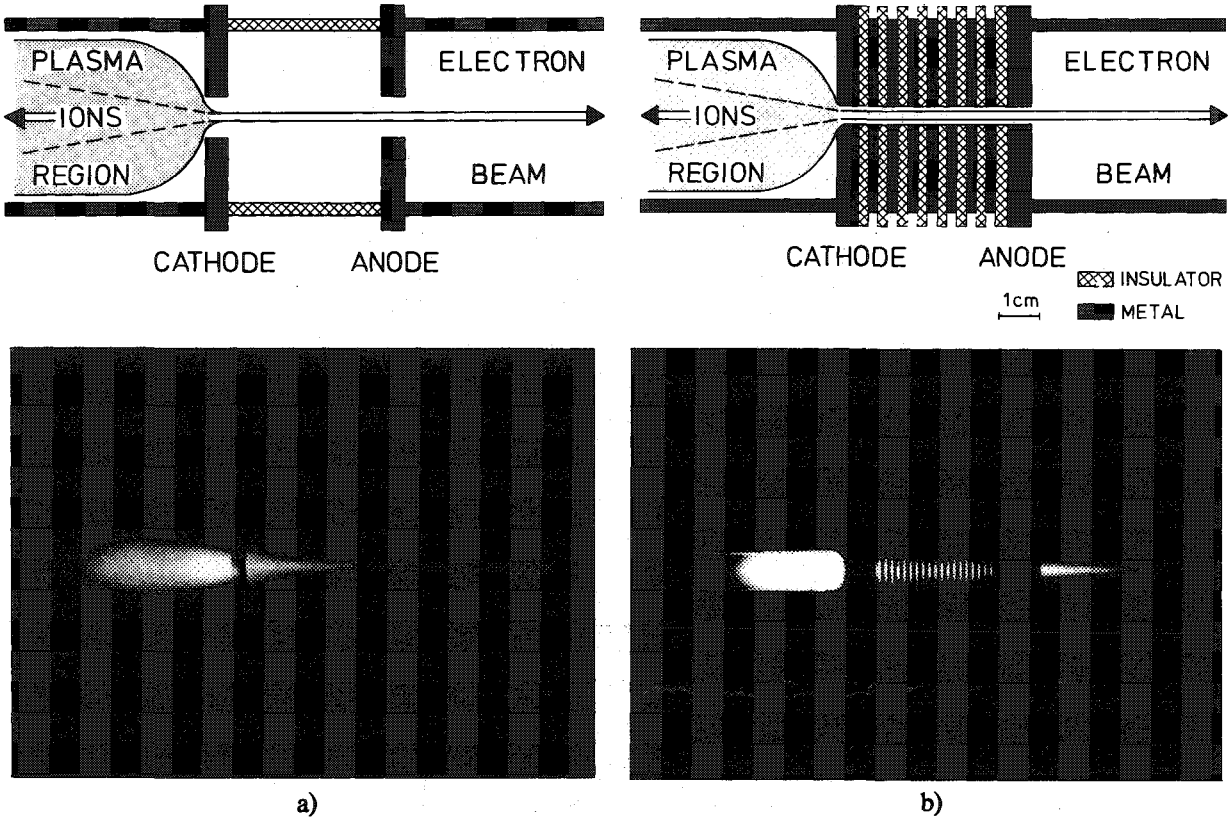

Fig. 4 Principle (top) and view (below) of a single-gap (a) and a multigap (b) pseudospark chamber

charge migration into this region. The plasma bubble may charge up to more than 100 V, thus forming a virtual anode (Fig. 5). The voltage breakdown is then induced by a rapid charge-carrier multiplication mechanism based on oscillating low-energy electrons [10] inside the virtual anode. Current rise-rates of up to 10^{12} A/s have been observed [4]. The current amplitudes also depend on the external electrical circuit parameters. The self-capacitance (20 pF) of a multigap PSC may deliver a short current pulse with amplitudes of more than 100 A, which is mainly the ejected electron-beam current.

It will remain a difficult task to explain fully the high current rise-rates observed in low-pressure pseudospark discharges of more than 10^{12} A/s, as well as current amplitudes of more than 200 kA. The slow propagation speed of the ionization front in the plasma bubble (10^6 cm/s) may be the reason for the relatively long formative time-lags, but not for the fast current rise in the discharge. The plasma temperature in the bubble has been measured between 10 and 100 eV. The plasma electrons will then have a speed of the order of 10^8 cm/s and could lead to the observed fast charge-carrier multiplication. The excellent trigger precision of the pseudospark discharge in switching applications is still unexplained.

The later stages of the pseudospark discharge—when electron and ion beams are formed in multigap PSCs, and magnetic forces act on the plasma in high-current switch discharges—have been studied and understood even less than the breakdown stage. From the measured currents and from the geometric dimensions, magnetic self-fields of several teslas are deduced. At this stage the discharge resembles a z-pinch discharge with the characteristic radial oscillations and instabilities of the axial plasma [11]. Generally, the ohmic resistance of the discharge channel decreases with increasing current and with time, hinting at a steady rise in the plasma temperature and a tendency to build up the plasma state that has the lowest inductance. Unlike in high-pressure discharges, the discharge channel has a diameter of the order of millimetres to centimetres. The current transition to the electrodes happens cylinder-symmetrically and over a rather large surface of several square centimetres (Fig. 6). Electrode heating and erosion are therefore small compared with what is seen in high-pressure discharges.

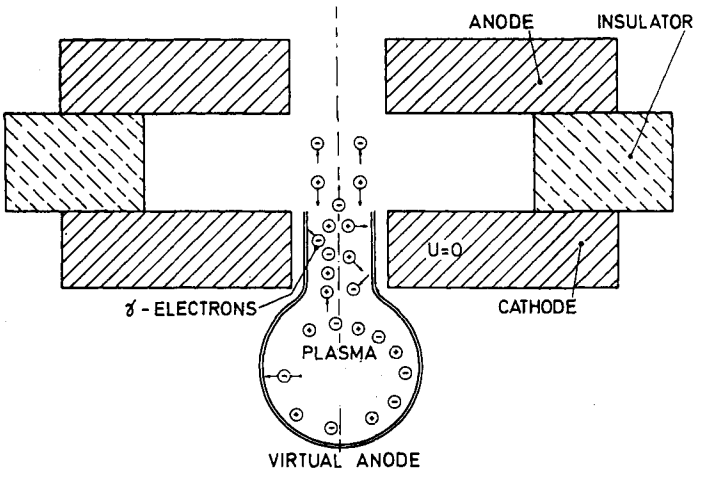

Fig. 5 Virtual anode formation in the hollow cathode of a pseudospark chamber.

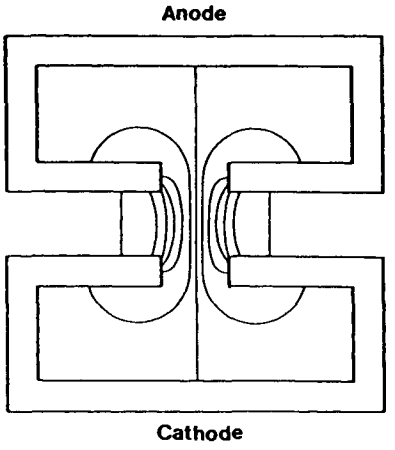

Fig. 6 Diagram of current flow in a single-gap pseudospark chamber

The phase after a pseudospark discharge is marked by a very fast recovery to the non-conducting state. Megahertz pulse rates have been achieved in multigap pseudospark discharges. Several reasons can be given for the rapid recovery: the small geometric dimensions of an almost fully metallic encapsulation of the discharge; the absence of heated electrodes and electron-emitting material; and the optional use of blocking electrodes which capture charge carriers. The good recovery rates also correspond to excellent voltage hold-off capabilities under clean conditions and with well-designed insulators. It is interesting to mention that a pseudospark discharge can even take place in a chamber where a low-current ($< 50\ \mu A$) d.c. discharge is occurring [12]. Apparently, almost the full voltage hold-off capability can be reached, even when not all charge carriers are eliminated from the main discharge volume. Although the physical processes of a pseusospark discharge cannot be described in detail, the prerequisites of a good switch are present, namely: good high-voltage stand-off capability in the non-conducting state; high trigger precision; high current rise-rate; low resistance in the conducting state; high current-carrying capabilities; smooth distribution of the current over a large electrode surface area; and fast recovery.

3. TRIGGER METHODS

3.1 General principles of triggering

The function of any switch trigger is to commutate the switch impedance from a very high value to a short circuit at a precisely defined moment. All electrical triggers for gas switches work directly

or indirectly by controlled injection of charges into the breakdown region. Electrons are generated by collisions and photoionization in the gas, or by γ-effect and surface discharges from metal and insulator surfaces. Only a *fast* charge-carrier multiplication effect can lead to a precise and rapid breakdown. In the case of low-pressure discharges, low-energy electrons—with their maximum ionization cross-section near 100 eV—are the most efficient. However, electrons alone are not sufficient. The low-pressure discharge can only develop out of a plasma. Such a plasma may be generated directly or indirectly from the ambient low-pressure gas or by evaporation of wall material. All the triggers for PSCs described below make use of the formation of a plasma bubble and of a virtual anode inside the hollow cathode. The trigger components are placed in the cathode hole, where they can be protected against damage from the main discharge. Laser triggering of PSCs [13, 14] also works with a low trigger energy and with an excellent precision; however, this method will not be dealt with here.

If the trigger is applied at the anode, an additional delay corresponding to the ion transition time from anode to cathode has to be taken into account. Triggering works equally well for single and multigap PSCs. Precisely triggered electron beam pulses have been generated with anode and cathode triggers [4, 15]. As in high-pressure discharges, the breakdown jitter has been shown to depend on the initial current of the charge carriers and on the distance of the trigger from the main discharge region. In case of the pseudospark discharge, the trigger delays are generally longer than in high-pressure discharges for the same amount of jitter.

3.2 Surface-discharge trigger

Surface-discharge triggers have long been used for high-pressure and vacuum spark gaps [16, 17]. In the first PSS built at CERN (in 1981), a trigger of this type was successfully used [4]. The principle of the trigger is shown in Fig. 7. One or two thin insulator disks of alumina, Mylar, or highly resistive carbon are embedded between the active trigger electrode and the electrode plates connected to the hollow cathode. A spark is initiated by an external pulse with amplitudes varying between a few hundred volts and a few kilovolts, and with a duration of 0.1 to 1 μs.

The mechanism of triggering can be described as plasma generation due to gas desorption and to insulator wall material evaporation produced by the surface discharge spark. Under the influence of the main field, this plasma ball is transformed, in a very short time, into a plasma 'bubble', which is characteristic of the pseudospark discharge under d.c. conditions near the self-breakdown limit. The high number of free electrons and of VUV photons may be responsible for the rapidity of the resulting main discharge. Typical values of delay-times between the arrival of the trigger pulse and the start of the main discharge are between one and several hundred nanoseconds, depending on the distance d_{trig} between the trigger spark and the main discharge gap. For low-power switches, the trigger insulator can be mounted inside the main gap on top of the cathode (Fig. 8), but it then has a shorter lifetime. As in all other types of gas switches, the jitter increases with increasing trigger delay.

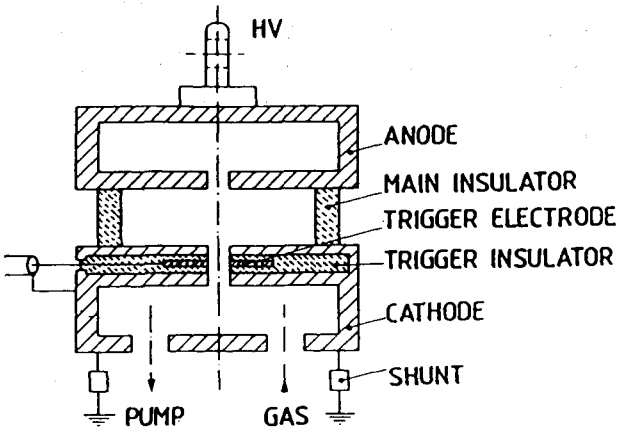

Fig. 7 Principle of a dielectric surface-discharge trigger

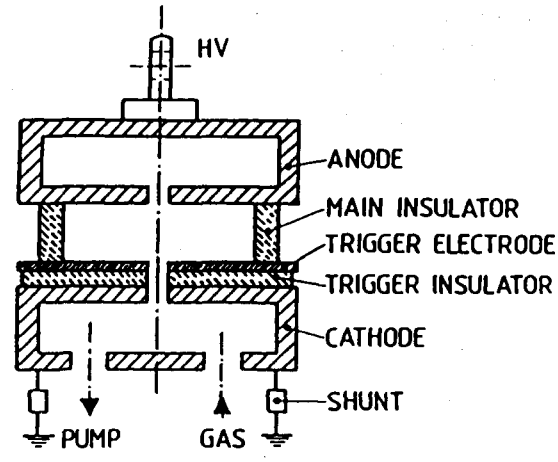

Fig. 8 Diagram of the surface-discharge trigger with the trigger electrode inside the main gap (highest possible switching precision!)

At delays below 30 ns, subnanosecond jitter values are obtained. For large d_{trig} (> 20 mm) the jitter rises to several tens of nanoseconds. Short trigger pulses with fast rise-times below 10 ns and amplitudes above 1 kV give the best results. The trigger-pulse energy may be smaller than 0.1 mJ!

When summarizing the performance of surface-discharge triggers for a PSS, the following advantages become evident:

- mechanical simplicity,
- no active elements, such as grids, in the main discharge region,
- no auxiliary voltages or currents,
- short switching delay,
- high precision, low jitter,
- simple external trigger-pulse circuitry,
- very low trigger-pulse energy,
- high current rise-rate.

The biggest disadvantage of a surface-discharge trigger is the limited lifetime due to the destruction of the trigger insulator by main and trigger-pulse energy. Another drawback is the evaporation of the trigger insulator material. Therefore, this trigger cannot be used in a completely sealed PSS. The most important applications are seen in experimental apparatuses which require simple but very fast and precise switching, and which have not to work for a long time in routine operation with high repetition rate.

3.3 Continuous electron-beam trigger

The continuous electron-beam trigger originated from experiments using a PSS with an auxiliary blocking-potential electrode inside the hollow cathode (Fig. 9). It has been shown [4] that a positive potential difference of a few volts with respect to the cathode can substantially increase the breakdown voltage of the system. Switching the potential of the auxiliary electrode from about 50 V to ground (or to a negative voltage) leads to breakdown of the main gap, provided the initial working point is chosen between the limiting breakdown curves belonging to each value of the blocking potential. The trigger energy of this simple system is negligible; however, delay and jitter are of the order of milliseconds. Hence the method is not practical for a real switch.

In order to enhance the trigger efficiency, we introduced a d.c. glow discharge of 1 mA, via another auxiliary electrode, from the rear of the cathode [12] (Fig. 10). This electrode is negatively charged to a few kilovolts with respect to the main cathode, which is at ground potential. The blocking electrode is normally held at a blocking potential of + 100 V. A low-density d.c. electron beam traverses the whole switch up to the main anode. Such high-energy electron beams do not significantly lower the voltage hold-off capability of the switch, provided 50 μA are not exceeded.

The breakdown of the main gap is initiated by switching the blocking potential from + 100 V to ground or to − 200 V. This leads to an expansion of the virtual anode inside the cathode, and to a deviation of a substantial part of the d.c. charge carriers from the blocking electrode towards the main cathode. The blocking-potential commutation can be achieved with a fast high-voltage transistor or a Reed relay. A 40 kV main-gap voltage has been switched, with 800 ns delay and 10 ns jitter, from a 25 Ω cable generator to a matched end resistor. Owing to the use of fast resonant charging, we could approach the self-breakdown limit very closely. Figure 11 shows the delay and jitter measurements of a system under steady high voltage.

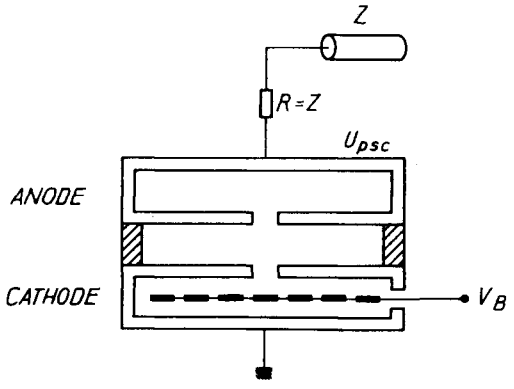

Fig. 9 Switching of a pseudospark switch by a blocking-electrode potential (V_B) commutation. Charging voltage = U_{psc}.

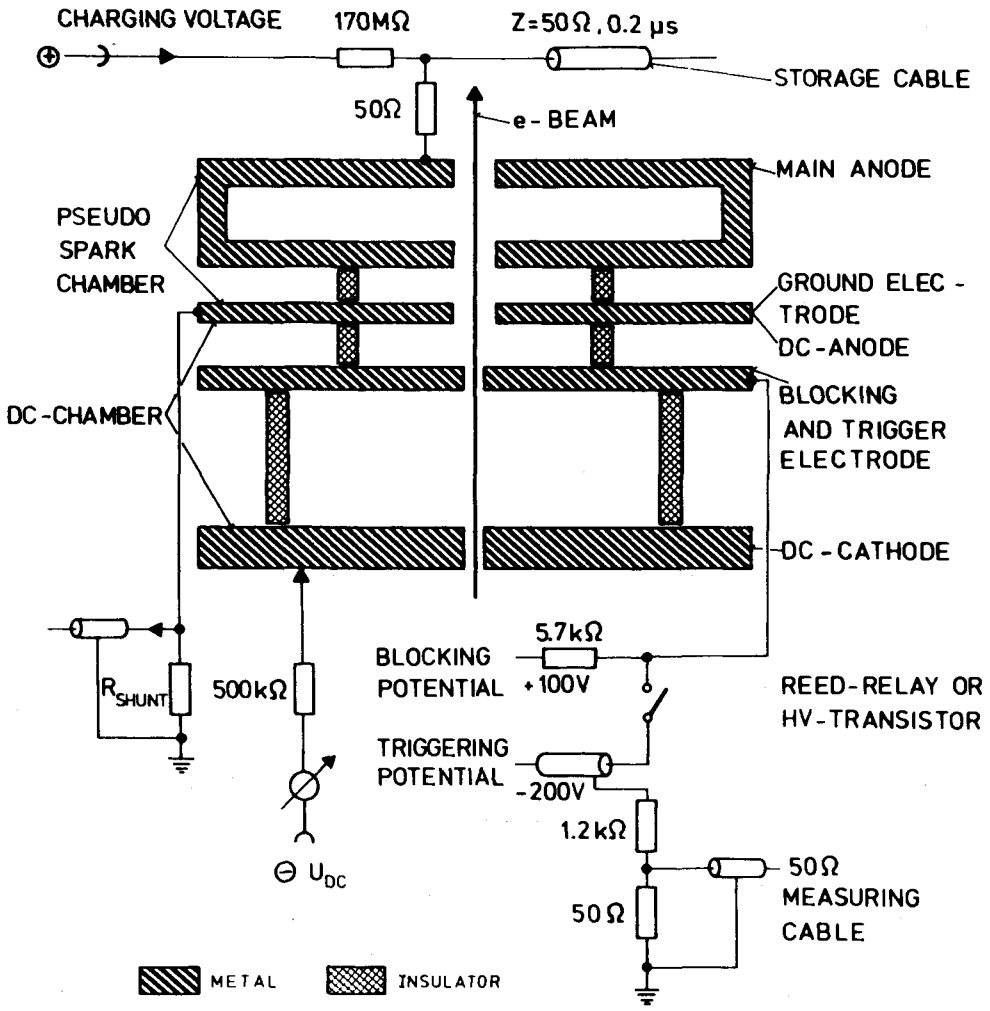

Fig. 10 Principle of the continuous electron-beam trigger

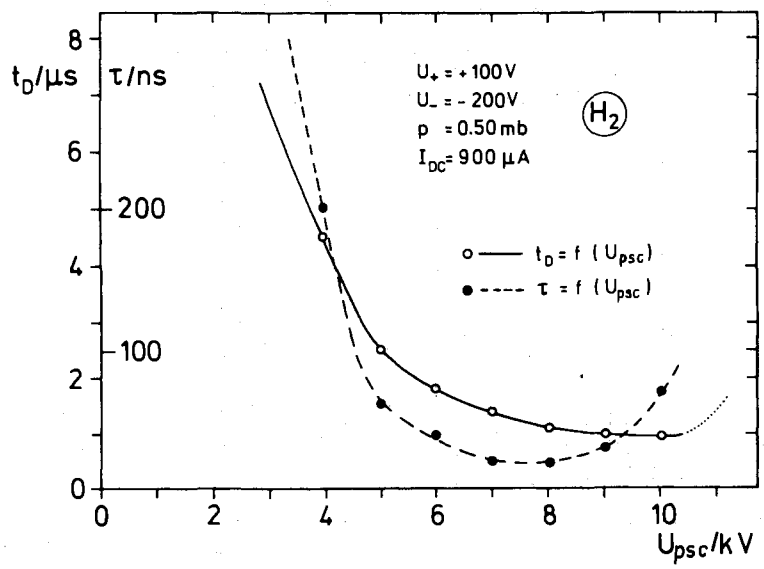

Fig. 11 Delay t_D and jitter τ as a function of voltage U_{psc} for the continuous electron-beam trigger

The continuous electron-beam trigger, which involves only simple metal electrodes and easily screenable insulators, is much more suitable for long-term operation than is the surface-discharge trigger. Since the trigger energy is small, very high frequency operation is possible. An extension of the principle to multichannel systems with a circular or a linear arrangement of the discharge holes is straightforward. Our first multichannel prototype switch had four holes on a circle of 1.5 cm radius. The four channels could be switched in parallel over a very narrow range of operating pressure and voltage. The essential requirement, which is that the jitter of the switch must be smaller than the voltage decay-time on the main gap, could be met only with considerable difficulty. The drawback of the continuous electron-beam trigger is its poor jitter and long delay time.

3.4 Pulsed electron-beam trigger

A pulsed *dense* electron beam with kinetic energy between a few hundred electronvolts and some kiloelectronvolts provides an easy and very efficient method of ionizing a low-pressure gas atmosphere. A single-gap or a multigap PSC, as shown in Fig. 4, may be placed behind the main cathode and be triggered to eject an intense electron beam ($\sim 10^{15}$ electrons per cm^3) through the cathode hole (Fig. 12). Such beams break down the main gap immediately. In this system the only jitter and delay come from the trigger of the auxiliary electron-beam PSC. Negative polarity on the far main electrode can be triggered almost equally well. Only an additional delay corresponding to the plasma transit time in the main gap has to be accepted.

Single-gap pulsed electron-beam triggers (Fig. 12) reach only a few tens of amperes but are almost as efficient. Jitter values of 1 ns have been measured for both types. The trigger range is very large and goes from the self-breakdown voltage down to a few hundred volts. Therefore, this trigger type can be applied in high-voltage and high-current switches. The sensitive parts of the auxiliary trigger are well protected from the power dissipated in the main gap.

3.5 Charge injection trigger

The poor precision of the continuous electron-beam trigger can be overcome by superimposing a pulsed discharge from an additional auxiliary electrode on the d.c. glow discharge at the desired moment of triggering. A variety of arrangements of trigger, blocking, and auxiliary electrodes are possible and have been partially studied. The original trigger system first proposed by Mechtersheimer et al. [18] is shown in Fig. 13. The main gap region is separated from the trigger

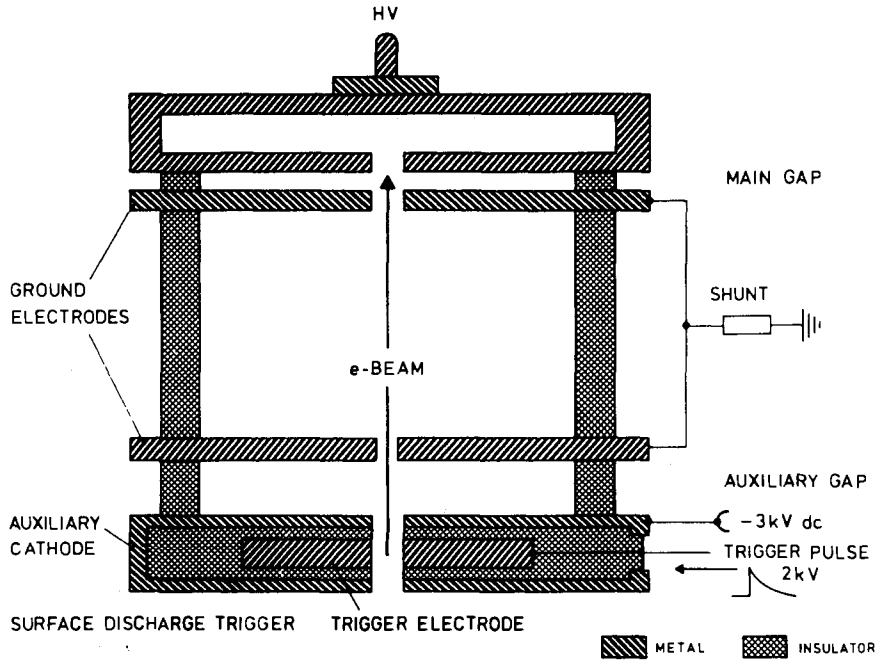

Fig. 12 Schema of a single-gap pulsed electron-beam trigger

system by a solid cylindrical cage which is part of the rear of the cathode electrode. The cage prevents high main currents and main plasma from penetrating the trigger region and damaging the trigger components. On the other hand, it considerably improves the current rise-time of the switch. Near the main cathode, a low-current (1 mA) flow discharge between auxiliary electrode 2 and ground provides pre-ionization, which extends weakly, through holes, into the interior of the cathode cage. A blocking potential of 300 V on auxiliary electrode 1 deviates most of the d.c. current from the cage; it also reduces the size of the virtual anode inside the cage by field penetration. Some hundred nanoseconds before triggering is desired, the blocking potential is switched to zero. Triggering then is initiated by a negative pulse of about 3 kV to the trigger electrode 3. After the main discharge, the blocking potential is reapplied. This leads to fast recovery and to efficient protection against pre-firing. The next discharge can be initiated within a few microseconds.

The charge injection trigger can also work without the blocking electrode 1 (Fig. 14). The price of the increased simplicity is, however, a diminished performance. To date, all charge injection

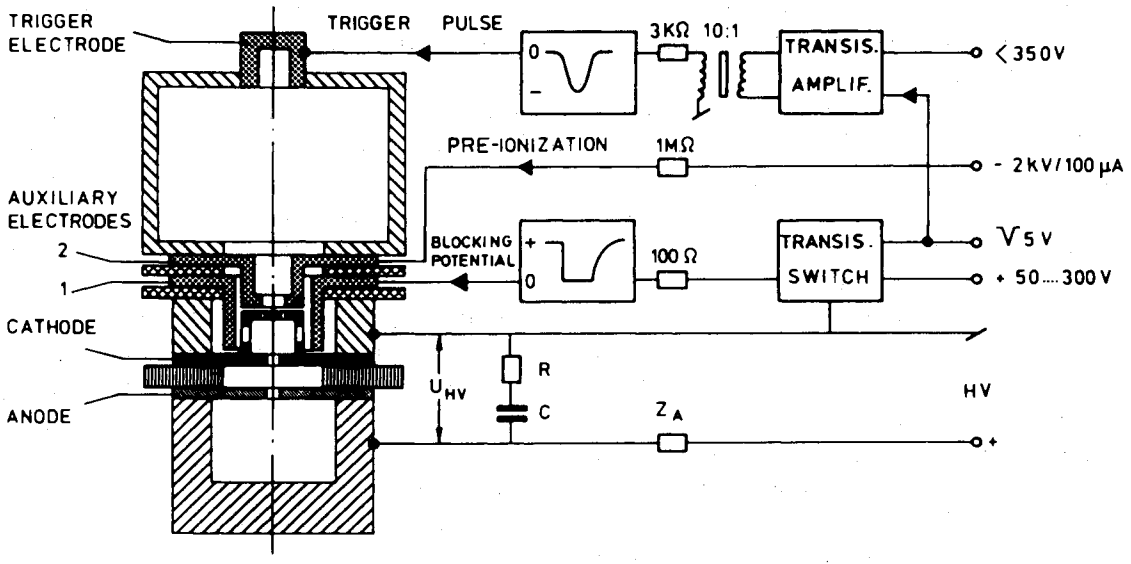

Fig. 13 Schema and electrical circuit of the charge-injection trigger (from Ref. [18])

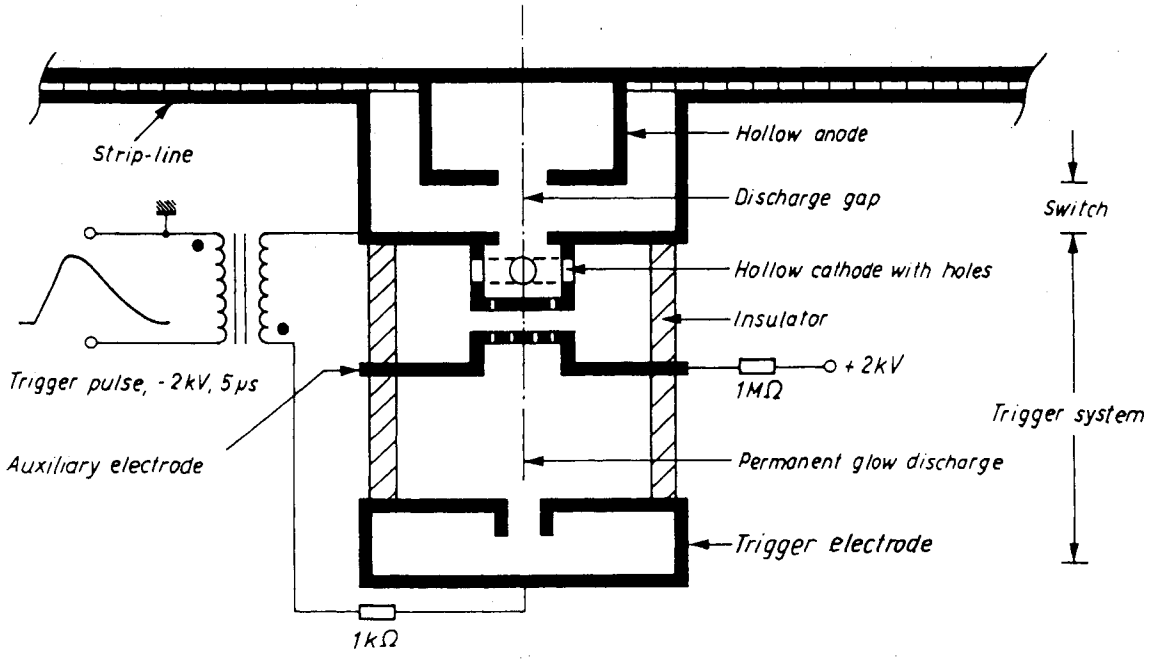

Fig. 14 Principle of a simplified charge-injection trigger for high-current pseudospark switches

trigger types studied feature rather long breakdown delays, between 0.2 and 2 μs. Nevertheless, subnanosecond jitter values are measured. The trigger range (i.e. the region between breakdown voltage U_B and lower trigger limit) depends strongly on geometry, d.c. discharge, and trigger pulse characteristics. The width varies typically between $U_B/2$ and 1 kV. Negative main polarity can be switched too, but with increasing delay and jitter. The charge injection trigger is ideal for multichannel switching [19]. The trigger itself shows neither erosion nor evaporation and is therefore very suitable for sealed switches.

4. MEDIUM-POWER SWITCHES

Medium-power switches are here defined as thyratron-like switches which work at circuit impedance levels above 1 Ω and which transmit pulse energies of much less than 1 kJ and charges of much less than 10^{-3} A·s. In this case negligible energy is dissipated per pulse inside the switch. The very first PSS (Fig. 3) was of this type. Other prototype switches were built which could be connected to any of the aforementioned trigger systems. All prototype switches were operated under variable gas pressure controlled by pumping speed and gas injection rate. This gave the necessary flexibility for the experiments and tests. There is, however, no reason why medium-power PSSs cannot be sealed off like thyratrons.

Cable pulse generators of 25 Ω impedance level were used. Different cable sets were available giving 100 ns, 400 ns, and 2 μs pulse lengths. The main objective of the investigations was not the optimization of certain switch and trigger configurations, but the search for geometries and parameter sets, such as pressure, d.c. ionizing currents, pulse currents, and synchronization times, which enabled safe switching with a comfortable operating range. Long-term runs served to find the weak points of switches and triggers.

The diagnostic comprised the main voltage measurement via the charging supply and a HV divider, a main current measurement by a 0.22 Ω shunt between switch and ground, and measurements of various auxiliary voltages and currents in the different trigger systems. In charge injection triggers, the operation of the blocking electrode potential is a sensitive means for studying the discharge and the recovery behaviour of the switch.

The first life-test with the first PSS was terminated after 5.5×10^6 pulses because oil had seeped into the main gap. In systematic long-term tests, several insulator materials and different widths of trigger insulator surface were tried. The thyratron trigger-pulse generator which delivered pulse amplitudes of 1.5 to 3 kV with a decay-time of 1 μs could be operated at a maximum repetition rate of 200 Hz. Slightly higher frequencies could be run with a transistor Marx generator [20], which delivered 1.5 kV pulses of 300 ns length. Most long-term tests were performed between 100 and 200 Hz. The original surface-discharge triggers were made with Mylar insulators of 0.3 mm thickness mounted on top of the cathode inside the main gap. None of the trigger insulators resisted more than 5×10^6 pulses under typical conditions of 20 kV charging voltage, 400 A current amplitude, and 2 μs pulse length. The initial jitter deteriorated after 10^6 pulses, from ±1 ns to ±2 ns (Fig. 15). A

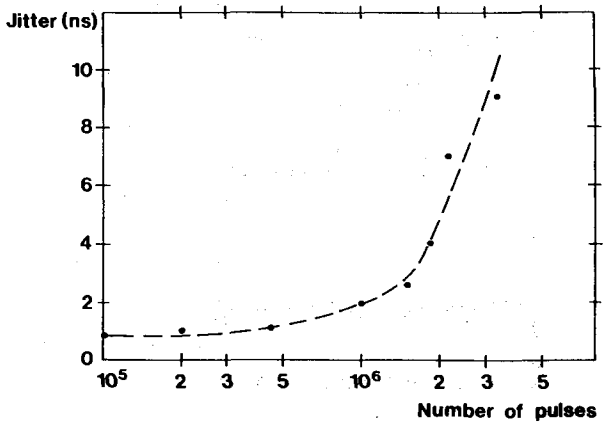

Fig. 15 Jitter as a function of the number of pulses for a pseudospark switch with a surface-discharge trigger switching 30 kV and 600 A and a 400 ns long pulse

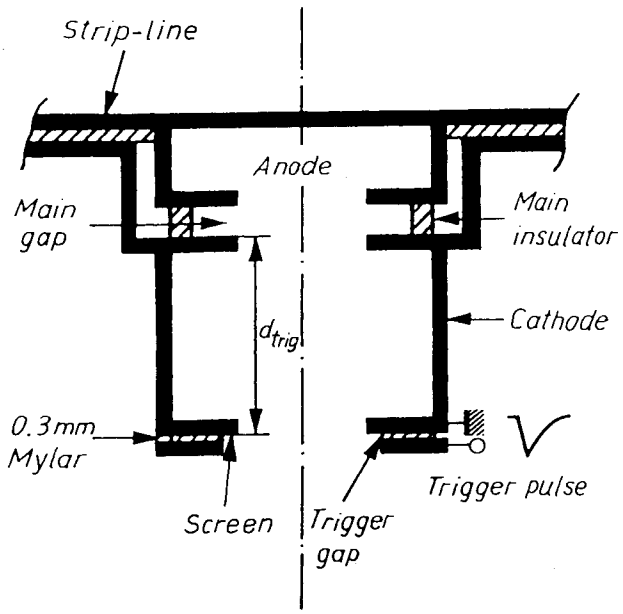

Fig. 16 Schema of the surface-discharge trigger for the high-current switch

considerable improvement of trigger lifetime was achieved by positioning the trigger electrode inside the hollow cathode (Fig. 16). This geometry improved the protection of the trigger and increased the lifetime of all materials by more than one order of magnitude. However, in all cases the jitter deterioration started after a few million pulses. The best long-term results were obtained with a highly resistive carbon material as the trigger 'insulator', which worked with a 1 μs trigger pulse at 25 kV, 500 A, and 400 ns pulse length for more than 1.5×10^8 pulses, but this material is mechanically very delicate to handle. Under the typical test conditions described above, and by shortening the trigger pulse length to about 100 ns, also Mylar and Vespel insulators reached lifetimes of 10^8 pulses.

The continuous and pulsed electron-beam triggers have been tested for several 10^6 shots but not up to the end of their life. The continuous electron-beam trigger has switched 40 kV in a resonantly charged pulse generator. The operating range of this type of trigger was very narrow in voltage, pressure, and repetition rate, the latter being limited to a few hertz. The pulsed electron-beam trigger performed well, so that a life-test would have been just another test of the Mylar surface-discharge trigger of the auxiliary PSC.

More studies have been carried out with several versions of the charge injection triggers. A trigger of the type shown in Fig. 13 has been pulsed for more than 10^8 pulses. Unlike the surface discharge triggers, the triggering and switching characteristics did not change during the test. The same results were obtained with the simpler trigger version shown in Fig. 14, which had also been implemented in high-current switches (Section 5). This trigger type is foreseen for application in a fully sealed-off medium-power pseudospark switch. Its jitter is, with a few nanoseconds, slightly worse than the jitter of the trigger with blocking potential electrodes, but the complexity of the total charge injection system is reduced.

5. HIGH-POWER, HIGH-CURRENT PSEUDOSPARK SWITCHES

5.1 Introduction

Since 1982, CERN has been working on the development of high-current switches which are needed in a special type of pulse generator, feeding current pulses of several hundred kiloamperes into powerful plasma lenses [21] to be used for secondary-particle collection at accelerator targets. Commercial peak-power switches featuring 20 kV hold-off capability, current intensities of more than 100 kA at a circuit impedance level of 20 to 100 mΩ, and repetition rates of 0.2 to 0.5 Hz, could not be found on the market. Peak-power switches on a pseudospark basis seemed particularly promising for this application.

A high-power switch is here defined as one in which a substantial part of the total pulse energy, say up to 10%, is dissipated inside it. This section will deal mainly with the characteristics, advantages, and problems of high-current PSSs. The results obtained with four PSSs in the above-mentioned 500 kA pulse generator will be reported and discussed.

5.2 Characteristics of high-power pseudospark switches

A PSS can be considered as a z-pinch structure with hollow electrodes, the holes of which are centred on the axis. However, in contrast to a z-pinch discharge where the current normally starts to flow at the insulator wall, the triggered pseudospark is always initiated on the axis. After transition of the pseudospark discharge into a z-pinch-like discharge, the rising azimuthal magnetic field helps to confine the current channel to the axis. The high density and temperature of the pinched plasma leads to a high conductivity, and hence to a low internal resistance of the switch. The insulator surfaces of the switch must be located far away from the discharge channel and have to be protected by metallic and dielectric screens.

The desired pinching of the current channel on the axis would be less favourable if it were to hit the electrodes in a small spot. Unlike in high-pressure spark gaps, the formation of craters in the electrodes is completely absent. The current density on the electrode surface is reduced by a factor of 10 compared with the density in the current channel in the gap. Therefore, the heating and the erosion of electrode material are small.

A consequence of the longitudinal geometrical symmetry of the PSS is that it is capable of sustaining full current and voltage reversals. Moreover, both charging polarities can be applied. Trigger systems can be positioned inside the hollow electrodes far away from the main gap, and can be well protected against hot plasma and leakage currents from the main discharge. As described in Section 3, very little energy is required to trigger a PSS precisely.

The specific pseudospark breakdown properties lead to fast current rise-rates. These rates are observed not only at small amplitudes but also at current levels above 100 kA. This means that after breakdown the fast initial rise is favourably backed up by the onset of a z-pinch-like dynamics with magnetic confinement and with a fast decay of plasma resistivity.

5.3 Triggers applied in high-power pseudospark switches

The general principles, mechanisms, and methods of trigger systems for the pseudospark discharge have been dealt with in Section 3. Here the special types of trigger that have been applied to high-current PSSs will be considered more closely.

A compromise has to be made between the efficiency and precision of the trigger system and its protection against the impact of current and plasma shock waves from the main discharge. The very high sensitivity of the pseudospark discharge for triggering from the hollow cathode allows us to obtain good precision and sufficient protection at the same time. A continuous d.c. electron-beam trigger (Fig. 10) has been experimentally used to switch 100 kA. This has been achieved with a pre-ionization current level of 10 μA and by commuting the potential of the blocking electrode from +100 V to zero. Owing to the tough environment, the characteristics of this trigger system were not very stable: the auxiliary voltages on the trigger electrodes and the switch pressure had to be frequently adjusted in order to maintain its switching capabilities.

Two additional and more resistant trigger systems have been operationally used in high-current PSSs. The first one is the simple surface-discharge trigger (Fig. 16). Near the main gap, a surface-discharge trigger would suffer severely. Metallization of the dielectric trigger insulator surface would result in a short circuit after a few shots through the main gap. Protection is easily provided by placing the trigger in the hollow cathode space and far enough away from the main gap, and by hiding it behind a screen (Fig. 16). As demonstrated in Figs. 17 and 18, the jitter and the delay increase with the distance d_{trig} between the trigger gap and the main gap, and additional protecting screens deteriorate the precision even more. The distance chosen is a compromise between precision and protection. Since the surface-discharge trigger works with a tiny spark produced by an external high-voltage pulse of a few kilovolts, it is also insensitive to electromagnetic interference from the very noisy environment.

The second type of trigger which has been used in a high-current PSS is a charge injection system similar to those described in subsection 3.5. Since long-term performance and simplicity are the main

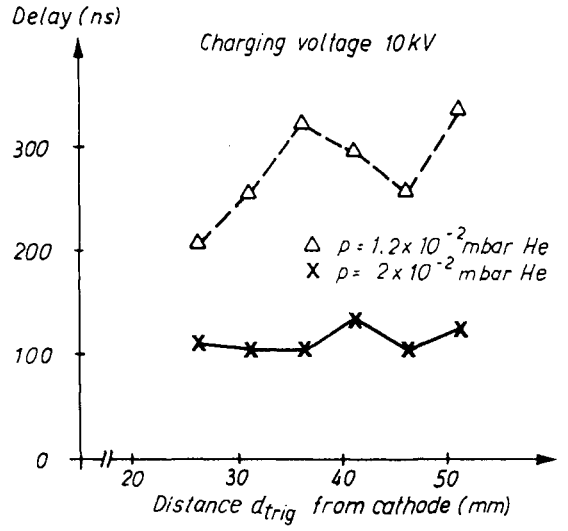

Fig. 17 Delay of the high-current pseudospark switch surface-discharge trigger at low (1 J) pulse energy as a function of the trigger distance from the main gap

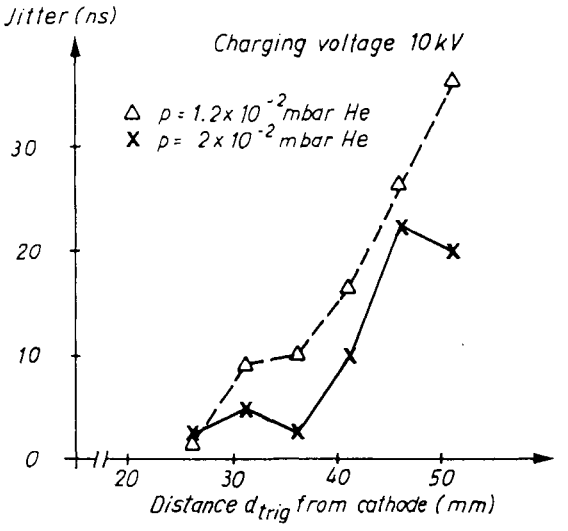

Fig. 18 Jitter of the high-current switch discharge at low (1 J) pulse energy as a function of the trigger distance from the main gap

objectives in a high-power, high-current switch, the most simple two-electrode configuration of a charge injection trigger has been chosen (Fig. 14). The total number of electrodes, including main anode and cathode, is four. This charge injection trigger can virtually not deteriorate. A very solid metal cage behind the cathode prevents the main current and the plasma from entering the rear volume, where a glow discharge is maintained between the auxiliary electrode and the HV trigger-pulse input electrode (Fig. 14). The voltage of a few kilovolts on the auxiliary electrode is positive, whereas the polarity on the trigger electrode has to be negative. Both auxiliary electrodes are of a simple shape and both are well protected from the main discharge. The same is true for all insulators in the hollow cathode space. The very good long-term behaviour, compared with that of the surface-discharge trigger, has to be paid for by the higher complexity of the additional d.c. glow-discharge voltage, which has to be stabilized. The amplitude and the duration of the high-voltage pulse superimposed on the glow discharge are of the same order as those of the surface-discharge trigger.

5.4 Design of a pseudospark switch for 100 kA

In the early stages of high-current PSS development, the prime importance of the discharge dynamics, the symmetry of the discharge, and the effects of electrode erosion and insulator attack were realized. In a high-power PSS the discharge is dominated by a hot-plasma column varying rapidly in diameter during the current pulse and interacting strongly with the wall material. The objectives in the design of a high-power PSS are therefore to maintain all the advantages of the initial stages of the discharge and, on the other hand, to provide the electrode and insulator geometries that are appropriate for plasma confinement and to choose appropriate materials, especially for where the main plasma–wall interaction takes place. Recent studies [21] of an imploding plasma-shell discharge have revealed the strong influence of the wall material, which is subject to direct contact with the plasma or to the strong radiation from the hot-plasma column. The wall material is not only lost by evaporation; under the impact of the energetic radiation from the central pinched column, ionization of the gaseous components near the wall leads to the onset of a wall current which then further enhances the evaporation of wall material. The thermal effects of plasmas on wall material have been investigated by several authors [22, 23]. A quality factor q can be calculated, for each material, from its thermal heat conductivity k, density ϱ, heat capacity C, and the evaporation or dissociation temperature T_{crit} as:

$$q = T_{crit} \sqrt{k \varrho C} . \qquad (1)$$

Classification with respect to q shows that insulators are generally much worse than metals and should be well protected from the direct impact of hot plasma and from radiation. Diamond and tungsten have the best q-factors. Hence, the choice of tungsten for the electrodes and screens of a PSS is a straightforward one.

Figure 19 shows the mechanical layout of a high-current PSS. The size of the metallic screens which encircle the discharge gap has to be such that the hot plasma cannot reach the main insulator region. At the same time the electrode distance has to be kept to the same value over the whole gap.

The diameter of the centre hole controls the amount of plasma that expands into the hollow electrode, and has to be such that the axial plasma is not laterally projected over the electrode screens. The axis of the centre hole should be the point with the lowest breakdown voltage in the switch. Long path breakdown in other regions has to be avoided. In order to favour the breakdown in the centre, the gas is injected into the cathode via the trigger system, and is pumped out through the main insulator. This generates a very favourable pressure gradient between the cathode and the insulator. At very high switched-pulse energies it is probably not advisable to work with a completely sealed-off switch at zero gas flow. Under such circumstances it will be difficult to maintain stable switching characteristics. During operation, the high-power switches are generally filled with helium at a pressure of 0.01 to 0.1 mbar, but they have been tested also with nitrogen and hydrogen.

During each pulse a considerable part of the switched energy is dissipated inside the switch when the total pulse-generator impedance is in the milliohm region. The centre parts of both electrodes are therefore strongly heated and must be water-cooled.

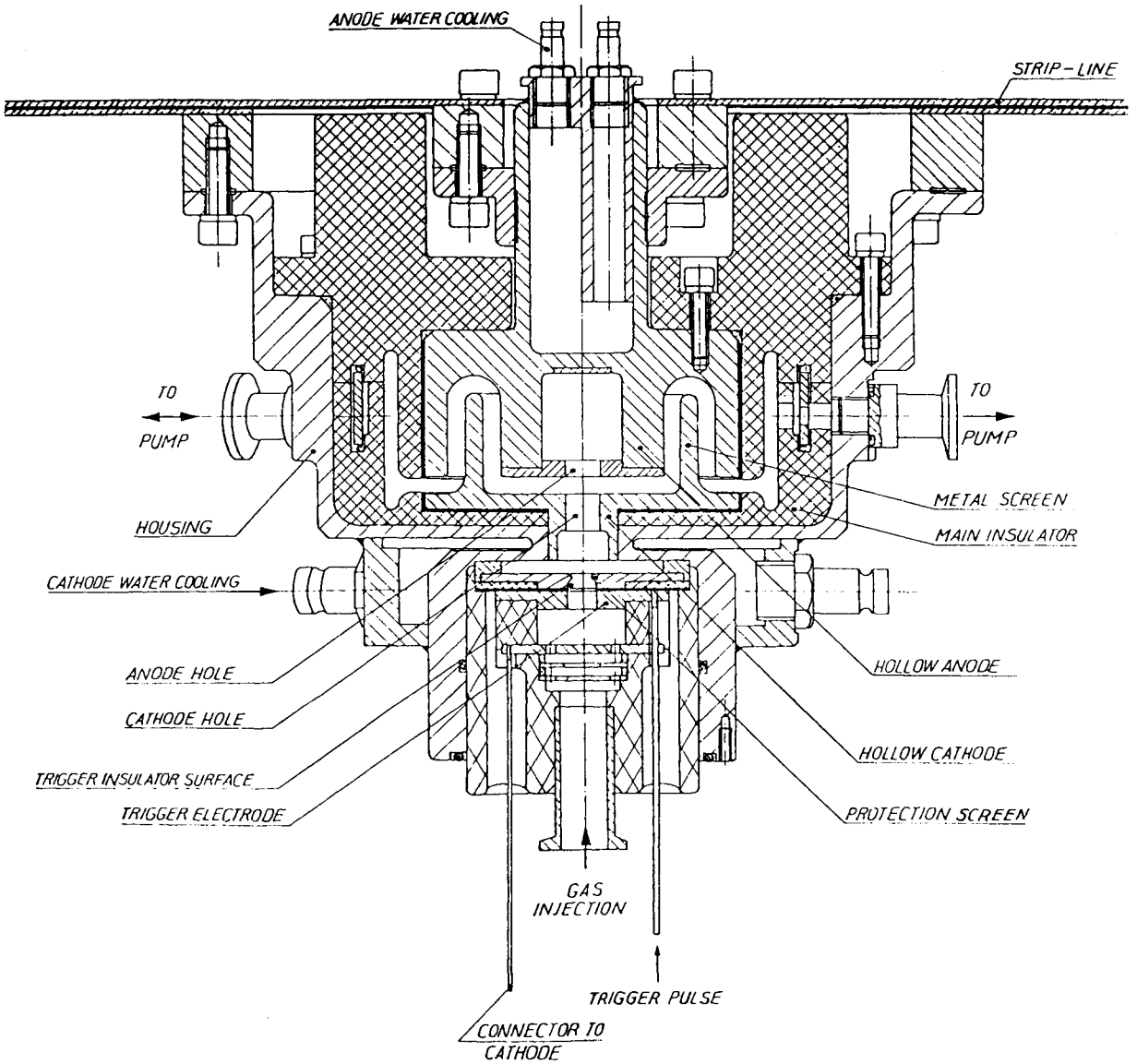

Fig. 19 Mechanical layout of the CERN high-current pseudospark switch

Four high-current PSSs, as shown in Fig. 20, have been installed in a 500 kA, 20 kJ pulse generator [24] intended for testing a plasma lens (Fig. 21). Each switch is mounted directly into a 600 mm wide strip line (Fig. 22). Modular trigger systems (Figs. 23 and 24) can be easily and quickly inserted into the high-current switches from the cathode side. Since, during the discharge, the whole switch swings up to a potential that is comparable with that of the charging voltage, all auxiliary components (such as vacuum pumps, trigger lines, and injection valves) linked to the switch have to be separated electrically from ground. Table 1 gives the features of the generator in which the high-current PSSs are used.

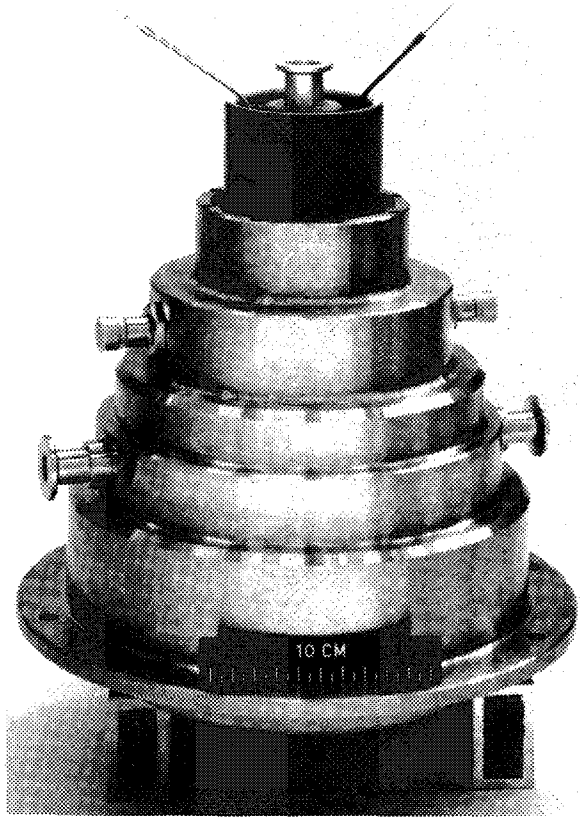

Fig. 20 Photo of the CERN high-current pseudospark switch

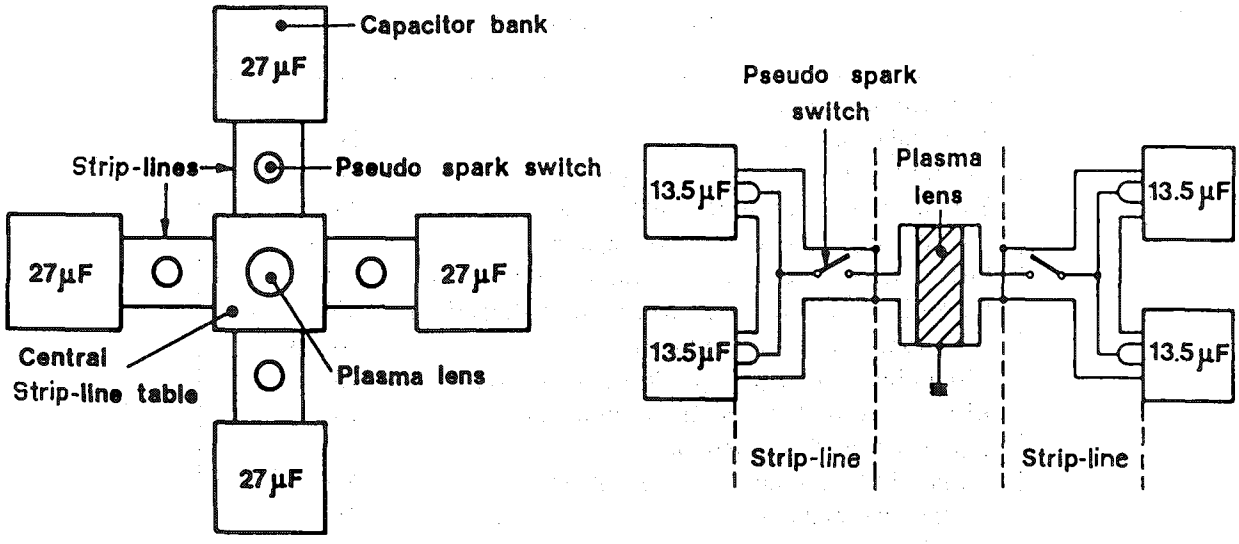

a) Top view b) Side view

Fig. 21 Schema of the plasma-lens pulse generator

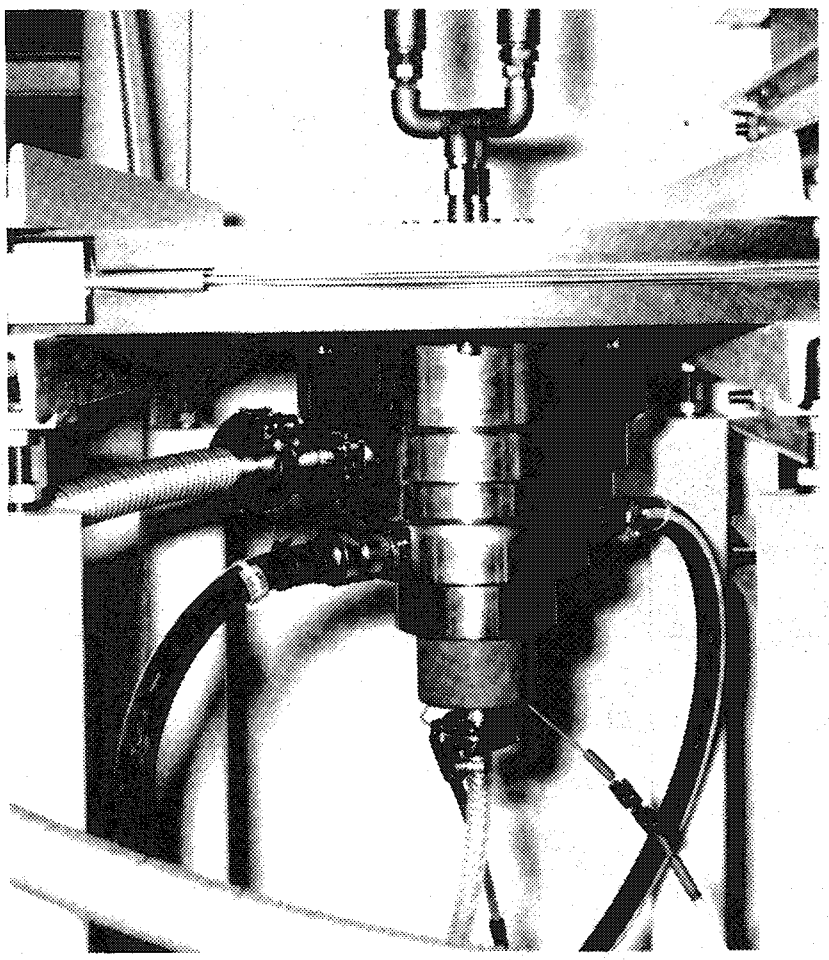

Fig. 22 High-current pseudospark switch mounted into the strip line of the plasma-lens pulse generator

Table 1

Pulse generator data

Capacitance, total (μF)	108
Nominal charging voltage (kV)	16
Maximum charging voltage (kV)	20
Stored energy at nominal voltage (kJ)	13.8
Stored energy at maximum voltage (kJ)	21.6
Peak discharge current at nominal voltage (kA)	400
Peak discharge current at maximum voltage (kA)	500
Inductance of plasma lens (nH)	20–100
Circuit inductance (except plasma lens) (nH)	13
Rise-time to first current maximum (μs)	1.6
Equivalent half-wavelength (μs)	7.4
Initial dI/dt at nominal current (A/s)	6×10^{11}
Voltage reversal (%)	45
Strip line cross-section (mm^2)	540×11
Distance between strip line conductors (mm)	0.9
Repetition period (s)	2.4

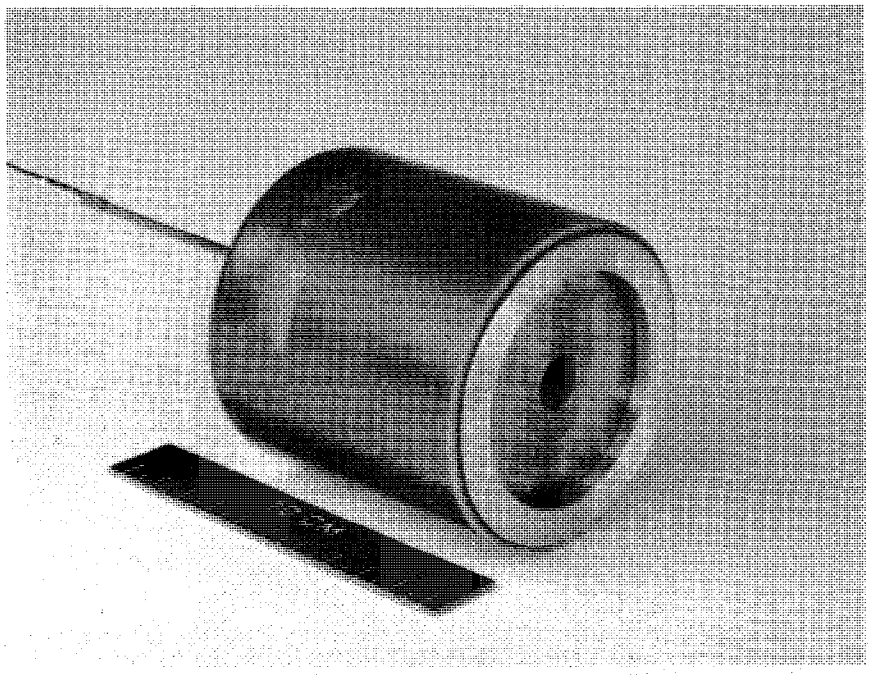

Fig. 23 Modular surface-discharge trigger for the high-current switch

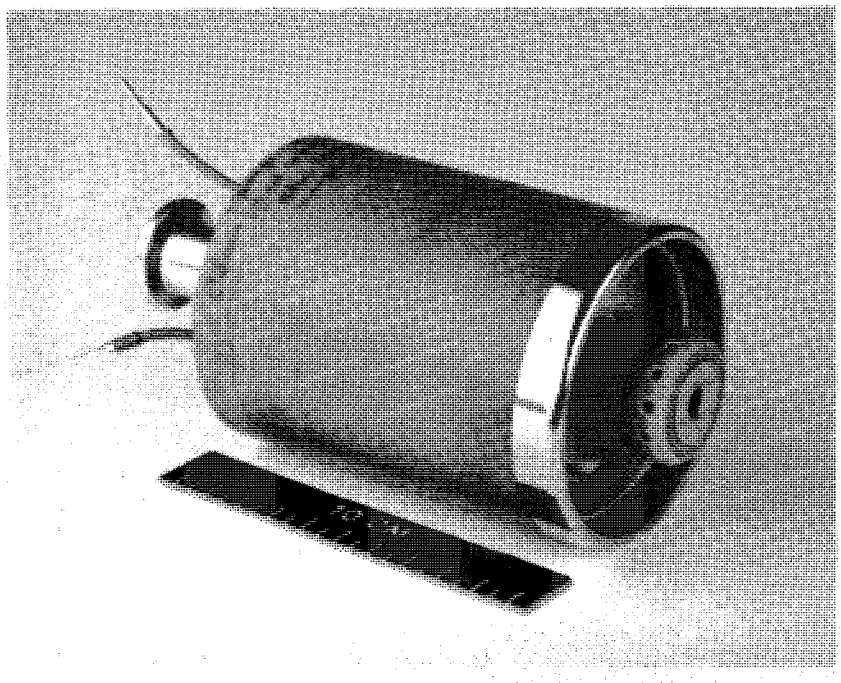

Fig. 24 Modular charge injection trigger for the high-current switch

5.5 Performance of the high-current pseudospark switches

Table 2 lists the main characteristics of the high-current switches. An essential requirement for their application in the plasma-lens pulse generator is the simultaneous switching of four pseudospark gaps, which can only be achieved when the breakdown delay of all four units can be made equal and when the jitter is smaller than the voltage decay-time on the switch. The total current

Table 2

High-current pseudospark switch features

Maximum hold-off voltage (kV)	> 25
Maximum peak current (kA)	200
Nominal hold-off voltage (kV)	16
Nominal peak current (kA)	100
Nominal charge transfer per pulse (As)	0.432
Reverse current (%)	100
Maximum dI/dt at 16 kV (A/s)	1.5×10^{11}
Switching delay (ns)	100–600
Jitter (pulse energy = 1 J) (ns)	± 10
Jitter (pulse energy = 3.5 kJ) (ns)	≤ ± 100
Inductance (nH)	40
Repetition period (s)	3
Filling gas	Helium
Gas pressure (mbar)	10^{-2}–10^{-1}
Electrode material	Densimet 18 (95% tungsten)
Insulator material	Araldite
Lifetime (shots at 3.5 kJ)	⩾ 400000

through the common plasma-lens load is shown in Fig. 25. The delay and the jitter of all four pseudospark switches are shown in Figs. 26a and 26b.

Depending on the gas pressure, the switches are operated with breakdown delays of 100 to 600 ns. The jitter of the high-current switch at high pulse power ranges from ± 50 to ± 100 ns. This is an increase of almost one order of magnitude compared with the jitter at low pulse power (Fig. 17). The precision is nevertheless sufficient to guarantee a good parallel switching of all four units. In order to avoid spurious breakdown, the switch is operated far from the breakdown curve (Fig. 27).

The current amplitude in each switch is normally about 100 kA when pulsing into the plasma-lens load. Occasionally, a current of up to 200 kA per switch has been pulsed with the same pulse generator through two different low-inductance short-circuit loads (Figs. 28a,b). In this case, current reversals of almost 100% were observed. A number of tests were performed to determine average values of internal resistance and inductance. The resistance values derived from the decrement of amplitude decay (Figs. 28a,b) are always higher than the value calculated for dI/dt = 0 (Figs. 29a,b). The typical average resistance at 100 kA is less than 1 mΩ (Fig. 30). Average dissipated energies in a single switch may reach 0.5 kJ (!) per pulse. An average internal inductance of less than 40 nH was derived from tests with different low-inductance short circuits. This value includes the

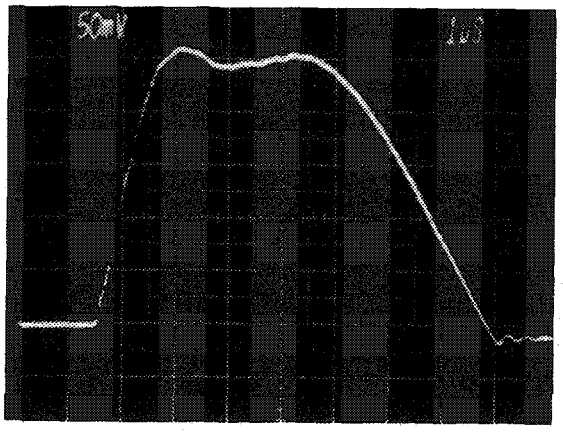

Fig. 25 Total plasma-lens current = sum of four pseudospark switch currents

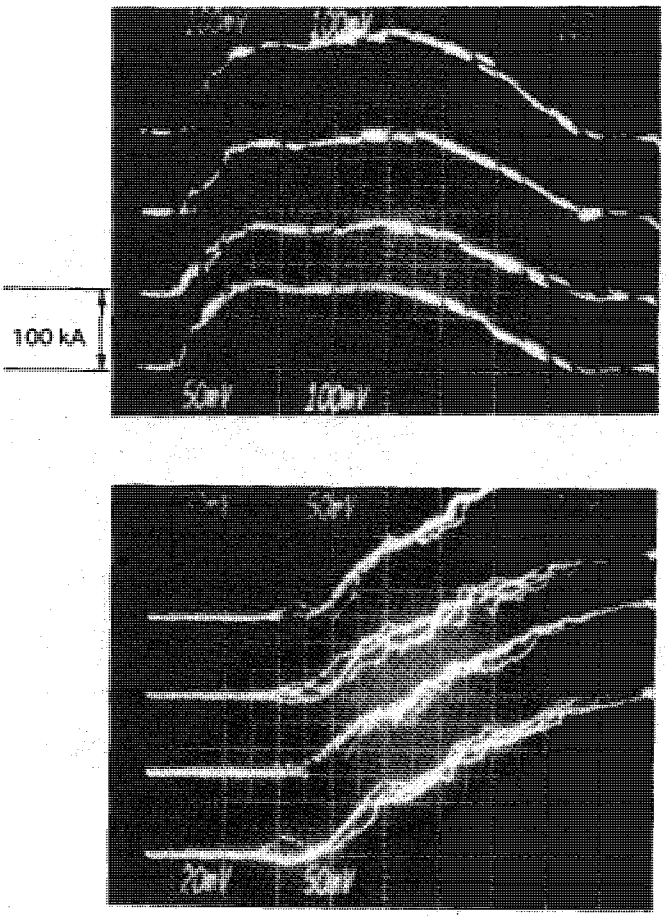

Fig. 26 Individual switch currents:
a) single shots, peak amplitudes = 100 kA;
b) 20 shots alternatively.

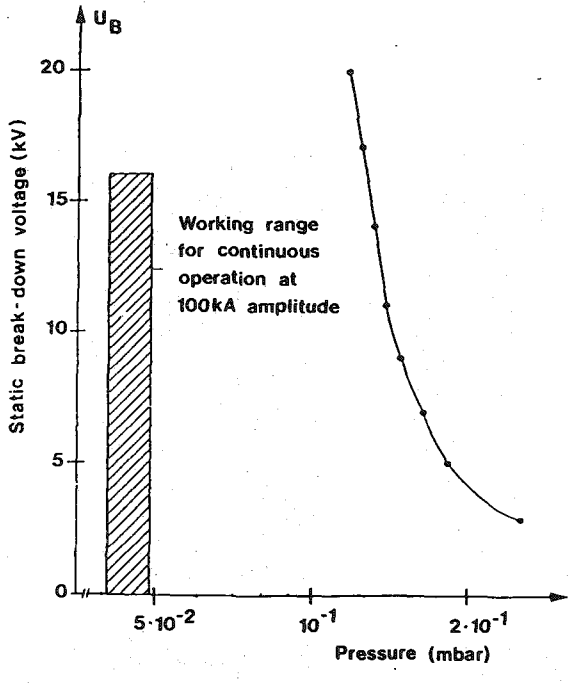

Fig. 27 Static breakdown curve and operating range of the high-current pseudospark switch

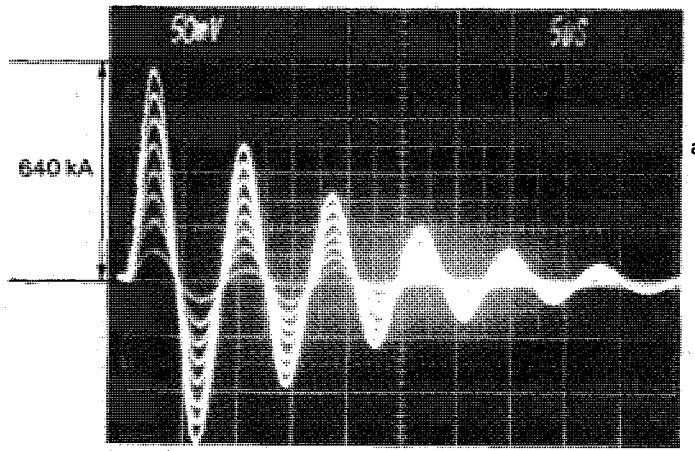

a) Charging voltages:
1, 2, 3, 4, 5, 6, 7, 8 kV

3.33 kA/mV
$\bar{R}$ = 1.7 mΩ (from decrement)

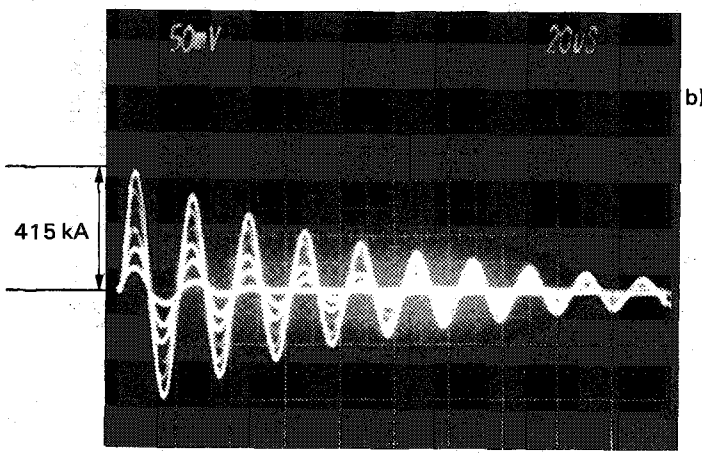

b) Charging voltages:
2, 4, 6, 8, 10, 12 kV

3.33 kA/mV
$\bar{R}$ = 2.2 mΩ

Fig. 28 Total current through a low-inductance short circuit:
a) load inductance = 5.5 nH; b) load inductance = 92 nH

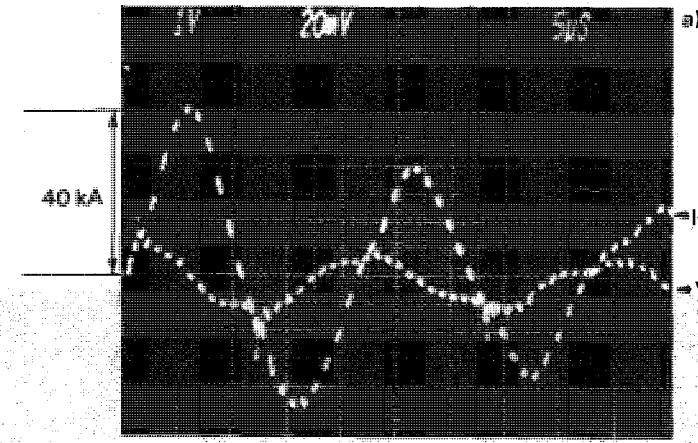

a) Charging voltage: 4 kV

0.66 kA/mV
1 kV/V

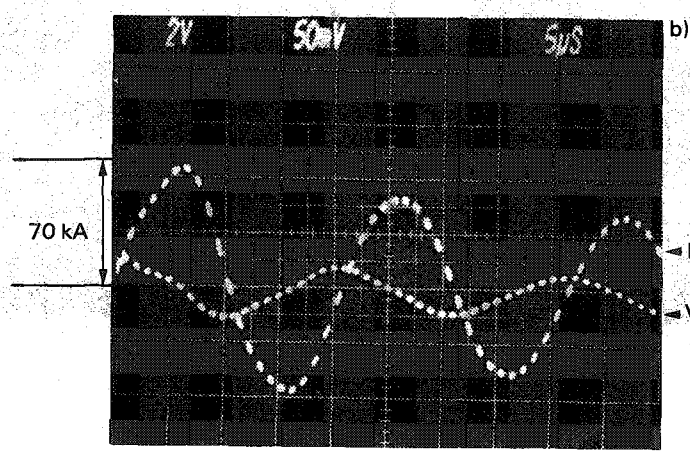

b) Charging voltage: 8 kV

0.66 kA/mV
1 kV/V

Fig. 29 Simultaneous voltage (V) and current (I) waveforms at a) low-current and b) high-current amplitudes showing higher losses at repolarization with low currents

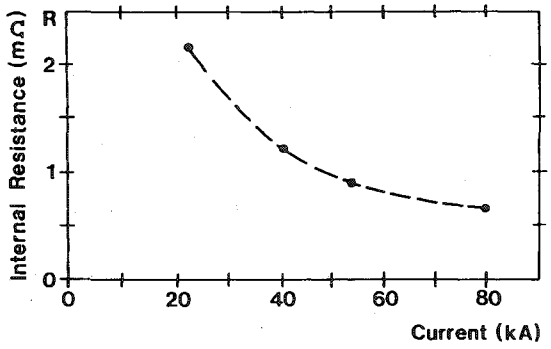

Fig. 30 Internal resistance of the high-current switch at peak current (dI/dt = 0).

connection between switch and strip line. The inductance of the four PSSs is the major contribution to the total external pulse-generator inductance of 13 nH.

Maximum current rise-rates of 1.5×10^{11} A/s were observed at a capacitor-bank charging voltage of 16 kV. Although this is the maximum rate observed with PSSs at such high current levels, the limitation of current rise is still given by the pulse-generator circuit characteristics and not by the switch itself.

The long-term performance of the four high-current PSSs has been studied during several life tests with the plasma-lens load. More than four hundred thousand pulses of 100 kA amplitude per switch have been pulsed every 3 s at 16 kV charging voltage without any remarkable deterioration of the switching properties. Inspection of one switch after 10^5 pulses revealed slight traces of erosion on the central electrode parts and on the metallic screen surface which is directly exposed to strong radiation from the plasma in the centre. The electrode surface was smoothly eroded, showing no crater formation or irregularity of discharge. The insulator, although composed only of organic components, was not attacked by the discharge. The delay and the jitter of the four switches had to be readjusted, after some ten thousand shots, by slightly changing the internal pressure on line, while keeping the breakdown delay equal in all four units. When the adjustment was done well, spurious breakdown rates far below 10^{-3} were observed. At the time of writing, the four switches are still performing successfully, and a lifetime of at least 10^6 pulses can be expected.

5.6 Summary

The capability of switching high-current, high-power, and high-pulse energy with pseudospark gaps has been clearly demonstrated in this section. In the high-current PSSs, current densities above 10^5 A/cm^2 have been achieved at very low impedance level. Cold hollow electrodes deliver apparently 10 to 100 times more current density than is delivered by heated cathodes. Demands for high current and power emerge not only from accelerator technology but also from high-power laser and inertial confinement fusion technology. Large primary stored energies are switched and compressed in successive stages before being transferred to the load, which may be a gas laser, a fusion pellet [25], or an accelerator gap [26]. Such systems need very precise and active primary switches that can transfer large amounts of electric charge, either directly or via the subsequent stages in which pulse compression takes place. This is done by means of passive or semipassive devices such as magnetic [27] or photoconductive switches [28]. The use of high-current, high-power PSSs as primary switches in such systems seems to be a big step forward in terms of better performance and less complexity.

Improvements to the high-power PSSs are mainly expected from the application of better electrode and insulator materials. The use of thoriated tungsten in the heaviest loaded electrode areas will result in an even smoother current distribution owing to the reduced electron work function, and therefore in less erosion. Inorganic insulator material with less outgassing rate will enhance the peak and average power-switching capability and will further reduce the spurious breakdown rate. Better performance is also expected from an optimization of the switch geometry, e.g. from a systematic matching of gap spacing, centre-hole diameter, hollow-electrode volume, cathode thickness, and screen diameter. The combination of optical triggers [13, 14] with high-current PSSs in multichannel mode may open up the way to the megampere region. Switches of this type could, in the future, replace the expensive magnetic switches in pulse compression systems for induction linacs.

6. HIGH-VOLTAGE SWITCHES

Only experimental high-voltage PSSs have been built so far. A study of the breakdown behaviour of one- and two-gap high-voltage PSCs was carried out in 1983 [12]. Figure 31 shows the experimental switch and Fig. 32 the electrical circuit. The switch was tested in a vacuum tank at a pressure of 10^{-6} mbar in order to insulate it from external flash-over. Straight cylindrical insulator rings of different dimensions and materials, such as glass and Macor, served to compose a variety of one- and two-gap configurations. The switch could be triggered by a surface-discharge trigger. Breakdown characteristics and jitter were determined as a function of insulator thickness, centre-hole diameter, gas type (N_2, He), polarity, and intermediate-electrode position.

Although at higher voltages the flashover across the insulator surface becomes the limiting factor, under clean conditions we observed that voltages of up to 130 kV were held by a single gap of 25 mm width, with a hole diameter of 3 mm at nitrogen pressures of 3×10^{-3} mbar or at helium pressures of 2×10^{-2} mbar. After some pulsing, the voltage hold-off capability of the insulators dropped. The jitter was measured for less than 5 ns in the whole range from 1 to 120 kV. The insertion of an intermediate electrode of floating potential into the main gap increases the breakdown voltage by a factor of up to 30 (Fig. 33). The enhancement is valid only in a limited pressure range and below 50 kV. At low pressures and high breakdown voltage, the insulator takes over and the enhancement effect disappears. In general, in the case of intermediate electrodes the breakdown curves are shifted to higher pressures. Higher breakdown voltages in the lower voltage and higher pressure range are obtained with a large upper gap (d_{up} = 12 mm) and a small lower gap (d_{low} = 3 mm). When the lower and the upper gap distance is comparable, the behaviour in the high-voltage range is improved. These effects can be explained by charge collection on the intermediate electrode modifying the field distribution in the chamber, so that in the small gap the field is considerably enhanced but is reduced in the long gap.

An operational high-voltage pseudospark switch can be built by applying proper electrode surface treatment and insulator shapes incorporating screening, so that the path length over the surface is at least ten times as long as the electrode gap distance. Tight sealing between electrodes and insulators is essential. Only then can one profit from the high field gradient of more than 100 kV/mm observed in multigap PSCs. High-voltage PSSs can also be composed of several single units in series. Laser-triggered PSSs [13, 14] are particularly well suited to such a series-connected system.

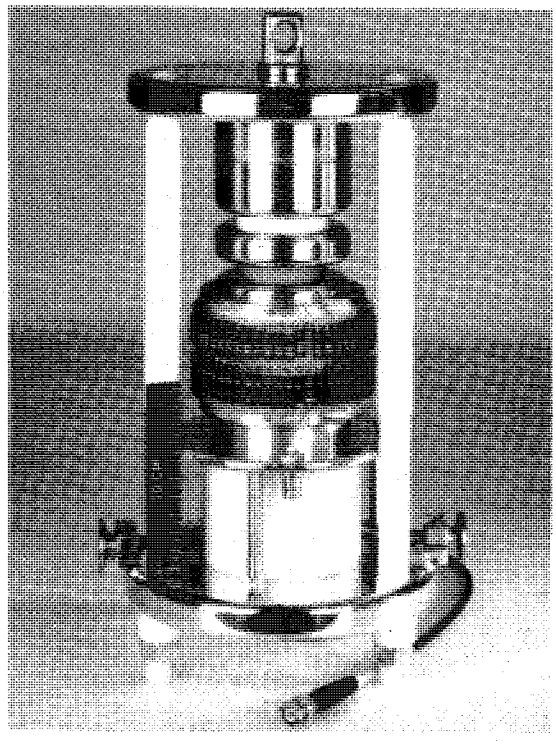

Fig. 31 High-voltage pseudospark switch prototype

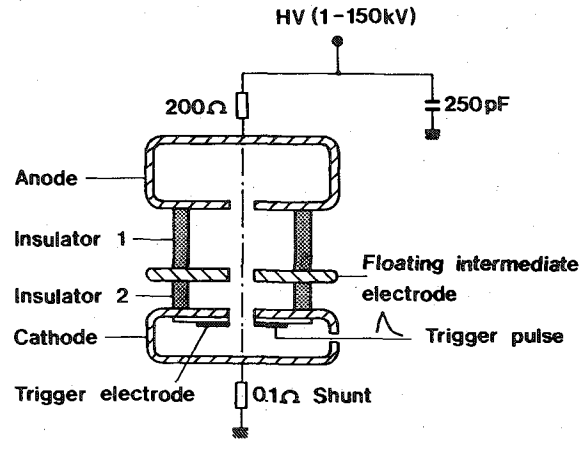

Fig. 32 Electrical scheme of the high-voltage pseudospark switch

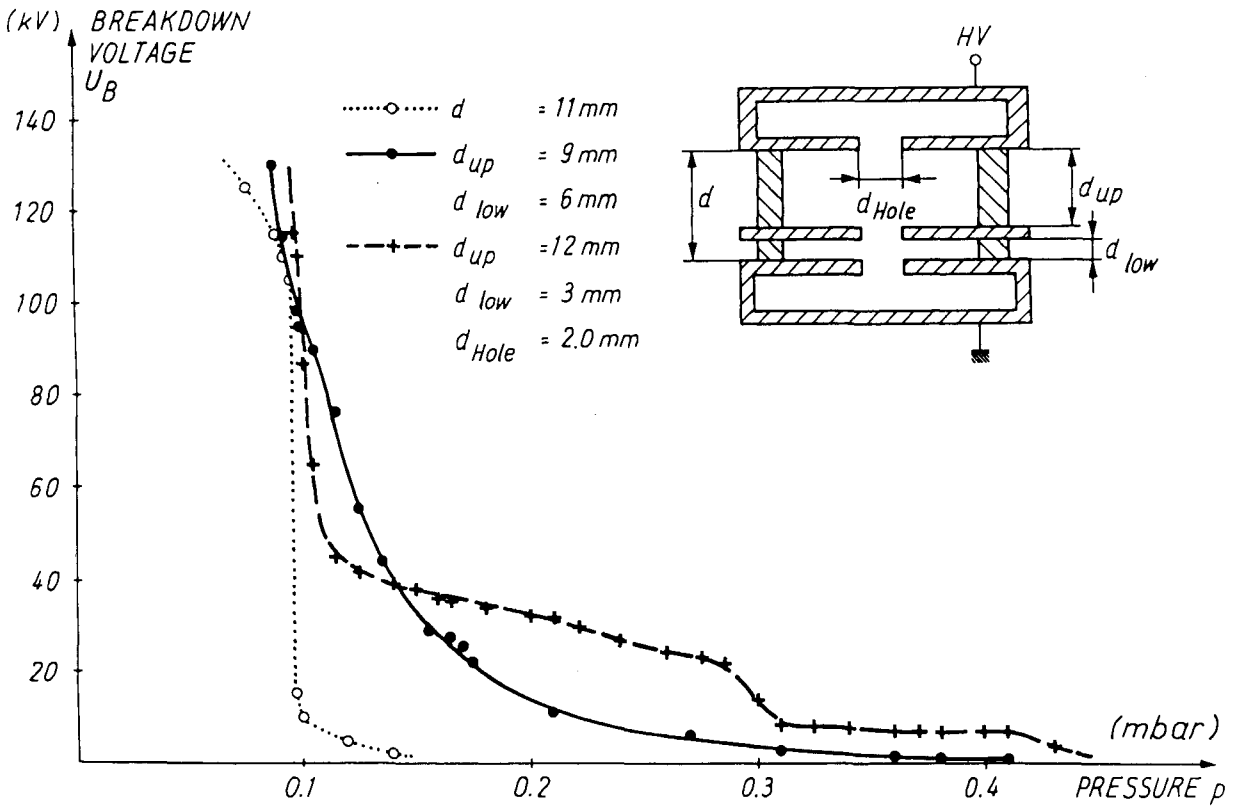

Fig. 33 Comparison of breakdown characteristics in a single-gap, high-voltage pseudospark switch with and without the intermediate electrode.

7. DISCUSSION OF AND COMPARISON WITH OTHER SWITCHES

7.1 Introduction

Before comparing PSSs with other closing switches, we will summarize the development reached up to now. High-current PSSs switch up to 200 kA and 2 A·s per pulse in the range of 1 to 20 kV with a precision of less than 50 ns jitter. Mechtersheimer et al. [18] achieved repetition rates of more than 100 kHz with single-channel, medium-power PSSs at 25 kV and 10 kA. Similar prototypes have been run [18] for more than 10^{10} pulses. With a 19-hole linear multichannel PSS (MUPS), Mechtersheimer et al. [19] obtained a current rise-rate of 2.4×10^{12} A/s at a voltage of 10 kV. At Kraftwerk Union, Erlangen, a 16-channel MUPS was built which featured 100 kA at 40 kV, with a pulse length of 200 ns and a repetition rate of 40 Hz. The current rise-time was 4×10^{12} A/s. Some of the most desirable requirements for high-power switching are [29]

- hold-off voltage up to hundreds of kilovolts,
- current-carrying capability of hundreds of kiloamperes,
- trigger voltage that is only a few percent of the operating voltage,
- jitter of the order of 1 ns or less,
- delay less than 20 ns,
- zero prefire and misfire probability,
- fast recovery to allow for kilohertz repetition rates.

In this section the PSS is compared with other gas-discharge switches. The question is, Which capabilities should be taken into account? The answer is difficult, as for most of the switches there exist a number of highly specialized versions that are optimized in one or two parameters at the expense of the rest. The work of Odom and co-workers [30] gives a good comparison of the maximum ratings of different switch types—including thyratrons, semiconductor switches, vacuum tubes, ignitrons, and high-pressure spark gaps—based on data sheets of commercially available tubes as well as on prototype tubes. In the preceding sections it was also shown that, with rather simple laboratory prototypes, the PSS reaches or exceeds the values of other gas-discharge switches. Table 3 gives some maximum ratings of the PSS together with data for thyratrons, ignitrons,

Table 3

Ratings that are characteristic of accelerator and high-power operation for switching tubes, compared with pseudospark switch prototype ratings reached up to now. Some data are only estimated.

	Pseudospark gap	Thyratron	Ignitron	High-pressure spark gap	Triggered vacuum gap
Maximum operating voltage gap (kV)	< 50	< 50	< 50	1000	50
Minimum trigger voltage (kV)	0.001 (!)	0.2	0.50	20	
Peak current (kA)	> 20 and 200 at low repet. rate.	~ 10	300 low repet. rate	1000	
Peak current density (A/cm^2)	10^5	10^3	10^4	$> 10^5$	$> 10^6$
Maximum pulse repetition rate (s^{-1})	10^5 at 1 kA	2×10^4	1	10^3 limited by gas flow-rate	Very low
Average current (A)	> 10	~ 25	Low	Low	Low
Max. charge per shot (10 μs pulse) (A · s)	2	$\sim 5 \times 10^{-2}$	200	5	2
Max. energy per shot (10 μs pulse) (kJ)	> 20	5–10	High	> 5	30
Minimum delay (ns)	1	50	500	30	
Min. jitter (ns)	0.4	< 1	50	< 1	
dI/dt (10^{11}) (A/s)	40	2	12	100	
Life (No. of shots)	10^{10}	10^{10}	Long	Low	Low
Cathode	Cold	Hot	Liquid Hg	Cold	Cold
High-voltage isolation required?	No (BLT)	Yes	Awkward	No	
Cathode life	Very long	OK for current within operating specifications	Very long	Short	Short
Conductive mode	z-pinch and glow	Glow	Arc	Arc	Arc
Fabrication simple?	Yes	No	Yes		
Gas flow	Low or none	Internal reservoir	None	High flow-rate	None
Forward drop	Very low	Low		High	High
Reverse current capability	100%	Life limit ~ 10%	No	100%. High erosion.	100%. High erosion.
References	4, 12–14, 18, 19	31–35	31, 36, 37	32–38	38

triggered high-pressure spark gaps, and triggered vacuum gaps, as taken from manufacturers' data sheets for commercially available tubes [4, 12–14, 18, 19, 31–38]. It is clearly seen from Table 3 that for certain applications the PSS can well serve as a substitute for expensive, established switch types, even in its laboratory version.

Table 4 shows the expected characteristics of future PSSs.

Table 4

Maximum projected ratings for future pseudospark switches

Voltage (MV)	1	Various parallel and series connections of single conducting channels (optically triggered, like BLT) [13, 14]
Current (MA)	2	
dI/dt (A/s)	10^{13}	In multichannel mode
Repet. rate (kHz)	> 100	Low power (10 J per pulse)
Life	$10^{11}/E_p$	E_p = Energy (J) per pulse. (Approximate scaling law for PSSs.)

7.2 General advantages of a pseudospark switch

- The PSS uses a very fast low-pressure discharge and therefore allows for a very rapid transition from the non-conducting to the conducting state.
- The well-defined position of the discharge channel minimizes the statistical time jitter.
- Current densities of more than 10^5 A/cm^2 can be withstood without narrow spark-channel formation. One channel can carry more than 200 kA total current.
- The pseudospark discharge can be effectively controlled from the interior of the hollow cathode and can be precisely triggered by a small number of charge carriers in this region.
- The simple geometry of the switch, with no auxiliary elements in the main gap, favours the design of high-voltage switches.
- The electrode holes and the location of the discharge channel defined by these holes lead to a smooth current transition and to a drastic reduction of erosion, as compared with plane electrodes.
- The simple geometry enables the tubes to be produced quite cheaply.
- The gas pressure in the switch is high enough to carry a large current without significant metal evaporation from the electrodes.
- The fast recovery after discharge allows high repetition rates.
- In multichannel mode, high current rise-rates of 4×10^{12} A/s are achieved.
- The current reversal in an oscillatory circuit represents no problem to the PSS owing to its nearly symmetric design with respect to the mid-plane of the gap.
- The switch can be used also in reversed polarity mode when surface-discharge triggers, charge-injection triggers, or optical triggers are used, because triggering works not only from the cathode region but also, with slightly higher delay, from the hollow gap.
- The switch in its basic version, with a surface discharge or an optical trigger, does not consume electrical energy in the standby mode and only very little with a charge-injection trigger.

All these features make the PSS a particularly easy-to-build, rugged, high-performance device. In the following subsections the differences between PSSs and other gas-discharge switches are discussed in more detail.

7.3 Pseudospark switches and thyratrons

Normally, thyratrons are used at medium power levels up to repetition rates of 10 kHz. The highest peak currents of 120 kA are reached by grounded-grid thyratrons; these use the thermionic

cathode as a source of trigger plasma that causes the breakdown of the short gap between grounded grid and anode [30]. Furthermore, there exist multistage thyratrons of up to eight staged gaps which can reach hold-off voltages of 240 kV [31]. Finally, there are double-ended thyratrons that use a cathode on both ends of the tube and are able to switch both polarities.

At the moment, thyratrons are the best developed gas-discharge tubes with the widest choice of types. From Table 3 it can be seen that, apart from special spark-gap switches, thyratrons offer the highest operating voltage of all commercially available tubes. The closed envelope allows very stable operation. Their switching precision is often better than 1 ns. However, the triggering grids are generally placed in the main discharge region.

The trigger voltage of thyratrons is low enough to use avalanche transistor Marx circuits as trigger generators. The pulse repetition rate may be as high as 50 kHz. The life expectancy of the tubes is of the order of 10^{10} cycles or more. Besides the positive points of thyratrons, there are also some drawbacks which are not present in other tubes, particularly in PSSs. Because of the complicated internal structure of thyratrons, they offer a hold-off voltage of only 30 kV to 40 kV per stage. To reach voltages in exesss of 100 kV a large number of stages are needed, but this has the disadvantages of greater cost, high inductance, and increased time jitter. In contrast, a two-stage PSC with well-designed insulators can already reach 120 kV hold-off voltage. The rather complex grid and baffle structures make a thyratron a relatively expensive tube. In heavy-load c.w. applications—as in lasers, in high-energy accelerators, or in airborne radar systems—a cheaper and simpler tube would be desirable.

Grounded-grid thyratrons are sensitive to the development of a concentrated spark channel [39] at high currents. When a spark develops, the tube falls into a quenched spark-gap mode. This already happens for a typical tube with a 10 kA, 10 μs pulse, limiting the charge per shot to 0.1 A·s. For very high current grounded-grid thyratrons that can carry 120 kA, the acceptable charge per shot is only 1.5×10^{-3} A·s [33], which means a pulse width of 12.8 ns. When the tube is quenched, a metal vapour arc develops. This leads to grid destruction, anode erosion, and, eventually, to hole drilling and loss of voltage hold-off capability. In the case of ceramic envelopes, it also leads to the production of oxygen from the walls.

Another disadvantage of thyratrons is their sensitivity to voltage reversal. This poses severe restrictions on their uses. No application is possible in oscillatory circuits. Also in pulse-forming networks, care has to be taken with the design.

Thyratrons employ at least two heaters, one for the thermionic cathode and the second for the hydrogen reservoir. This permanent source of energy consumption requires at least some tens of watts of heater power per tube or hundreds of watts in high-power tubes. The presence of plasma in a thyratron leads to a non-zero probability for a prefire. In the basic version of the PSS, there is negligible consumption of energy and less tendency to misfire.

7.4 Pseudospark switches and ignitrons

The ignitron types used today are mostly metal-envelope tubes with an insulated graphite anode and a mercury-pool cathode. Ignitrons can carry the largest current of all commercially available tubes [37] and also large amounts of charge per shot (see Table 3). Their lifetime may be reduced by permanent ringing operation. Ignitrons are triggered by comparatively low voltages, typically 1 kV, and are therefore accessible to transistor or thyristor triggering.

A weak point of the ignitrons is the poor switching precision [40]. The formation of the hot spot and glow discharge at the ignitor–mercury interface requires of the order of 500 ns, and the resulting jitter amounts to 50 ns or more, even when a control grid is used. A PSS is more suitable in those high-current switching applications where exact timing is required, e.g. for pulsed magnetic lenses in particle accelerators.

Not only the ionization time but also the de-ionization and cool-down times are very long, so that in a high-current ignitron the allowable repetition rate may be as low as one shot per minute; therefore a fast repetitive operation, such as can be achieved with PSSs, is impossible. With an ignitron, one has to be very careful that no negative voltage swing occurs at the ignitor while the tube is in a conducting stage, because this will deviate the arc to the ignitor, which is then rapidly destroyed.

7.5 Pseudospark switches and high-pressure spark gaps

There exists a large variety of triggered high-pressure spark gaps. The trigatron-like spark gaps have the trigger electrode integrated axisymmetrically in one of the main electrodes [39]. These have the shape of half-spheres, and use longitudinal triggering between the trigger electrode and the opposite electrode. They can handle large currents at high voltage levels [41]. Another spark-gap type uses an intermediate torus-shaped trigger electrode which is mounted axisymmetrically between the two main electrodes. The application of a voltage pulse to this electrode causes one part of the main gap to break down, the other following after a short delay.

Most of the spark gaps described in the literature are prototypes that are not commercially available. In particular, in pulsed-power research and magnetic-fusion experiments, dedicated spark gaps are developed for every single experiment [42]. The voltage and the current range up to several megavolts and megamperes. Different types of pre-ionization schemes are employed, such as corona discharge and laser and UV irradiation. Spark gaps are usually triggered electrically, but there exist an increasing number of laser-triggered spark gaps. Laser triggering reduces the delay time and the jitter, but this requires a powerful laser and makes the switch much more expensive.

High-pressure spark gaps easily sustain increased current levels, but only at the expense of increased electrode erosion. In a PSS this erosion is less, owing to the absence of a narrow discharge channel. High-pressure spark gaps that are carefully designed can hold off a large voltage per gap. They can also accept inverse currents without being damaged, and can well be used in oscillatory circuits. The current is not limited by the gas pressure in the gap—as it may well be in low-pressure devices, particularly when the plasma erosion cannot be compensated for by the diffusion of new neutrals. The spark-gap switches are easy-to-build, rugged devices that do not contain complex grid structures. Their sensitivity to damage is therefore less than that of other tubes.

On the other hand, high-pressure spark gaps show very severe electrode erosion in high-current switching. This erosion increases the fluctuations in the location of the discharge spark channel, which in turn leads to increased jitter. It also limits the permissible repetition rate of the spark-gap switch. The location of the current path in a PSS is defined by the axis of the tube, and remains there even in the presence of electrode erosion. Another difference between the PSS and the high-pressure spark gap is the narrow and relatively long discharge channel in this gap, which limits the possible rate of current rise owing to high inductance.

Perhaps the most serious disadvantage of triggered high-pressure spark gaps is the obvious dependence of their switching precision on the charging voltage. A reliable triggering is only achieved for a voltage range between $0.3U_B$ and $0.8U_B$, where U_B denotes the self-breakdown voltage of the gap. To achieve low jitter (< 5 ns) and a delay of the order of 30 ns, an operating voltage of at least $0.7U_B$ should be used. This strong dependence of the timing properties on the operating voltage level makes high-pressure spark gaps difficult to use in applications where switching synchronization on a nanosecond time-scale is required.

The trigger voltage for a high-pressure spark gap needs to be much more than for a PSS—of the order of 50% of the operating voltage for low-jitter operation. Some commercially available high-pressure spark gaps even need 100% of the operating voltage as trigger. The consequence is that a large number of stages are required to trigger a high-voltage gap, which in turn means that expensive trigger generators have to be used, and which also limits the repetition frequency.

7.6 Pseudospark switches and triggered vacuum gaps

Only a small number of triggered vacuum gaps are commercially available, and no complete set of data for these tubes can be found in the manufacturers' sheets [38]. The currents in these gaps are not specified, but the maximum energy per shot value and charge per shot value are similar to those of the PSS (see Table 3). The triggered vacuum gaps offer a very wide range of operating voltages, which compare favourably with those of pseudospark gaps. A typical figure is an operating voltage from 0.3 kV up to 50 kV. Triggered vacuum gaps are comparable to PSSs in several respects, but the latter still have the advantages of reduced electrode erosion, owing to their geometry, and better triggering characteristics, owing to the presence of low-pressure gas.

8. CONCLUSIONS

The rapid progress in PSS development has already resulted in a significant extension of high-power switching technology. Pseudospark switches combine the advantages of different conventional switches such as thyratrons, ignitrons, and spark gaps. In gas-laser technology, the high current rise-rates of PSSs can push the power limits up by at least one order of magnitude. Accelerator technology can profit from faster magnets pulsed at higher repetition rates. Pseudospark switches are attractive for future fast-rising and fast-cycling extraction systems of damping rings in linear colliders. They are also interesting for switched-power linacs and induction linacs, free-electron lasers, and accelerators for inertial confinement fusion. They can replace primary and magnetic switches in pulse compression systems.

The development of PSSs, which had started in 1981 at CERN, is an impressive example of the 'spin-off' of high advanced technology to industry. The pseudospark research continues, and the industrial production of PSSs is already envisaged in France, Germany, and Japan.

The successful development of this new technology will hopefully incite the accelerator community to support the work being done in other new, promising, plasma and pseudospark-based technologies for high-density particle beam sources and for the generation of ultra-high electric and magnetic fields.

Acknowledgements

The authors are very much indebted to J. Christiansen and H. Schopper who, in 1982, initiated the co-operation between the University of Erlangen–Nürnberg and CERN and the research and development work on pseudospark switches. We thank R. Billinge, E. Jones, and all people in the PS Division who supported us during the last five years, when the Division was heavily charged with the construction of three more machines: LIL, EPA, and ACOL.

We are also grateful to the CERN EF Division, especially to R. Grüb who provided us with space and equipment for the first high-current switch tests.

We thank M.A. Gundersen and D. Möhl for reading the manuscript and making valuable suggestions.

REFERENCES

[1] J. Christiansen, Z. Angew. Phys. **4** (1952) 326.

[2] F.W. Büsser, J. Christiansen, H.P. Hermsen, F. Niebergall and G. Söhngen, Z. Phys. **187** (1965) 243.

[3] J. Christiansen and C. Schultheiss, Z. Phys. A **290** (1979) 35.

[4] D. Bloess, I. Kamber, H. Riege, G. Bittner, V. Brückner, J. Christiansen, K. Frank, W. Hartmann, N. Lieser, C. Schultheiss, R. Seeböck and W. Steudtner, Nucl. Instrum. Methods **205** (1983) 173.

[5] V. Brückner, Dr. Arbeit, Univ. Erlangen-Nürnberg (1984).

[6] G. Bittner, J. Christiansen, W. Dümmler, N. Lieser, R. Seeböck and W. Steudtner, Spectroscopic investigation of the pseudospark discharge, Contribution to the Symp. on Atomic and Surface Physics '84, Maria Alm (Salzburg), 1984.

[7] J. Christiansen, N. Lieser, W. Rath, W. Steudtner, K. Rozsa, M. Janossy, P. Apal and P. Mezei, Opt. Commun. **56**, No. 1 (1985) 39.

[8] W. Neff et al., Verhandl. DPG (VI) 20, Vortragsnr. P-VII, P61, Vortrag an der Frühjahrstagung 1985 der DPG, Bayreuth (1985).

[9] P. Röhlen and F. Müller, Verhandl. DPG (VI) 21, Vortragsnr. K-III, K16, Vortrag an der Frühjahrstagung 1986 der DPG, Stuttgart (1986).

[10] H. Helm, Z. Naturforsch. **274** (1972) 1812.

[11] F. Dothan, H. Riege, F. Boggasch and K. Frank, J. Appl. Phys. **62** (9) (1987) 3585.

[12] J. Christiansen, K. Frank, H. Riege and R. Seeböck, CERN/PS/AA/83-22 (1983).

[13] G.F. Kirkman and M.A. Gundersen, Appl. Phys. Lett. **49** (9) (1986) 494.

[14] K. Frank, E. Boggasch, J. Christiansen, A. Goertler, W. Hartmann, C. Kozlik, G.F. Kirkman, C. Braun, V. Dominic, M.A. Gundersen, H. Riege and G. Mechtersheimer, High-power hollow electrode thyratron-type switches, presented at the 6th IEEE Pulsed Power Conf., Washington DC, 1987.

[15] H. Riege, CERN/PS/86-8 (AA) (1986) and CERN CLIC Note 14 (1986).

[16] L. Caris and E.M. Williams, CERN 69-13 (1969).

[17] J.M. Lafferty, Proc. IEEE **54**, No. 1 (1966) 23.

[18] G. Mechtersheimer, R. Kohler, T. Lasser and R. Meyer, J. Phys. **E19** (1986) 466.

[19] G. Mechtersheimer and R. Kohler, J. Phys. **E20** (1987) 270.

[20] J. Christiansen, K. Frank and W. Hartmann, Nucl. Instrum. Methods Phys. Res. **A256** (1987) 529.

[21] B. Autin, H. Riege, E. Boggasch, K. Frank, L. De Menna and G. Miano, IEEE Trans. Plasma Sci. **PS-15** (1987) 226.

[22] R. Behrisch, J. Nucl. Mater. **93 & 94** (1980) 498.

[23] C.B. Wheeler, J. Phys. **D7** (1974) 546.

[24] E. Boggasch, V. Brückner and H. Riege, Proc. 5th IEEE Pulsed Power Conf., Arlington, Va., 1985 (85C 2121-2 of IEEE Catalog, New York, 1985), p. 820.

[25] B.N. Turman, T.H. Martin, E.L. Neau, D.R. Humphreys, D.D. Bloomquist, D.L. Cook, S.A. Goldstein, L.X. Schneider, D.H. McDaniel, J.M. Wilson, R.A. Hamil, G.W. Barr and J.P. VanDevender, *ibid.*, p. 155.

[26] D. Birx, E. Cook, S. Hawkins, S. Poor, L. Reginato, J. Schmidt and M. Smith, IEEE Trans. Nucl. Sci. **NS-30**, No. 4 (1983) 2763.

[27] W.C. Nunnally, Los Alamos Nat. Lab. report LA-8862-MS, Rev. 2 (1984).

[28] W.C. Nunnally, Los Alamos Nat. Lab. Progress report LA-10360-PR (1985), p. 25.

[29] D. Turnquist, R. Caristi, S. Friedman, S. Merz, R. Plante and N. Reinhardt, IEEE Trans. Plasma Sci. **PS-8** (1980) 185.

[30] H.B. Odom, T. Burkes, M.M. Kristiansen, W. Portnoy, M. Lager and J.P. Craig, Proc. 2nd Int. Conf. on Energy Storage, Compression and Switching, Venice, 1978 (Plenum Press, New York and London, 1983), p. 987.

[31] Hydrogen Thyratron Product Data, English Electric Valve Co. Ltd., Chelmsford, UK (1982).

[32] Power Grid Tubes, Thomson CSF, Division Tubes électroniques, Catalogue DTE 045, Paris (1976).

[33] Ceramic Metal Grounded-Grid Thyratrons, EG & G Electro-Optics, Data Sheet H 5003D-1, Salem, Mass. (1980).
[34] Ceramic Metal Hydrogen Thyratrons, EG & G Electronic Components, Data Sheet H 5010A-1, Salem, Mass. (1983).
[35] Ceramic Metal Hydrogen Thyratrons, EG & G Electro-Optics, Data Sheet H 5000C-4, Salem, Mass. (1980).
[36] Ignitron Product Data, English Electric Valve Co. Ltd., Chelmsford, UK (1983).
[37] Ignitrons, G-E Tube Products Department Publication M-1256, Shenectady, NY (1974).
[38] EG & G Electro-Optics Short Catalogue, Salem, Mass. (1983).
[39] H. Menown, Proc. First IEEE Int. Pulsed Power Conf., Lubbock, Texas, 1976 (IEEE, New York, 1976?), p. IA2-1.
[40] N. Warmoltz, The Time Lag of an Ignitron, Philips Res. Rep. **6** (1951) 388.
[41] B.R. Gray, High-Energy Switch Device Study at RADC, Proc. 12th Modulator Symposium, New York, 1976 (IEEE, New York, 1976), p. 51.
[42] D.R. Humphreys, K.J. Penn, J.S. Cap, R.G. Adams, J.F. Seamen and B.N. Turman, Proc. 5th IEEE Pulsed Power Conf., Arlington, Va., 1985 (85C 2121-2 of IEEE Catalog, New York, 1985), p. 262.